

UNIVERSIDAD DE CONCEPCIÓN



CENTRO DE INVESTIGACIÓN EN
INGENIERÍA MATEMÁTICA (CI²MA)



A posteriori error analysis of an augmented fully-mixed
formulation for the non-isothermal Oldroyd-Stokes problem

SERGIO CAUCAO, GABRIEL N. GATICA,
RICARDO OYARZÚA

PREPRINT 2017-25

SERIE DE PRE-PUBLICACIONES

A posteriori error analysis of an augmented fully-mixed formulation for the non-isothermal Oldroyd–Stokes problem*

SERGIO CAUCAO[†] GABRIEL N. GATICA[‡] RICARDO OYARZÚA[§]

Abstract

In this paper we consider an augmented fully-mixed variational formulation that has been recently proposed for the non-isothermal Oldroyd–Stokes problem, and develop an a posteriori error analysis for the 2D and 3D versions of the associated mixed finite element scheme. More precisely, we derive two reliable and efficient residual-based a posteriori error estimators for this problem on arbitrary (convex or non-convex) polygonal and polyhedral regions. The reliability of the proposed estimators draws mainly upon the uniform ellipticity of the bilinear forms of the continuous formulation, suitable assumptions on the domain and the data, stable Helmholtz decompositions, and the local approximation properties of the Clément and Raviart–Thomas operators. On the other hand, inverse inequalities, the localisation technique based on bubble functions, and known results from previous works, are the main tools yielding the efficiency estimate. Finally, several numerical results confirming the properties of the a posteriori error estimators and illustrating the performance of the associated adaptive algorithms are reported.

Key words: Oldroyd–Stokes problem, non-isothermal, stress-velocity formulation, fixed-point theory, augmented fully-mixed formulation, mixed finite element methods, a posteriori error analysis

Mathematics subject classifications (2000): 65N30, 65N12, 65N15, 35Q79, 80A20, 76R05, 76D07

1 Introduction

We have recently introduced an augmented-mixed finite element method to numerically approximate the flow patterns of a non-isothermal incompressible viscoelastic fluid described by the non-isothermal Oldroyd–Stokes equations [6]. The underlying model consists of the Stokes-type equation for Oldroyd viscoelasticity, coupled with the heat equation through a convective term and the viscosity of the fluid. The original unknowns are the polymeric part of the extra-stress tensor, the velocity, the pressure, and the temperature of the fluid. In turn, for convenience of the analysis, the strain tensor, the vorticity, and the stress tensor are introduced as further unknowns. This allows to join the polymeric and solvent viscosities in an adimensional viscosity, and to eliminate the polymeric part of the extra-stress tensor

*This work was partially supported by CONICYT-Chile through BASAL project CMM, Universidad de Chile, project Anillo ACT1118 (ANANUM), project Fondecyt 11121347, and the Becas-Chile Programme for Chilean students; by Centro de Investigación en Ingeniería Matemática (CI²MA), Universidad de Concepción; and by Universidad del Bío-Bío through DIUBB project 151408 GI/VC.

[†]CI²MA and Departamento de Ingeniería Matemática, Universidad de Concepción, Casilla 160-C, Concepción, Chile, email: scaucao@ci2ma.udec.cl.

[‡]CI²MA and Departamento de Ingeniería Matemática, Universidad de Concepción, Casilla 160-C, Concepción, Chile, email: ggatica@ci2ma.udec.cl.

[§]GIMNAP-Departamento de Matemática, Universidad del Bío-Bío, Casilla 5-C, Concepción, Chile, and CI²MA, Universidad de Concepción, Casilla 160-C, Concepción, Chile, email: royarzua@ubiobio.cl.

and the pressure from the system, which, together with the solvent part of the extra-stress tensor, can anyway be approximated later on by postprocessed. In this way, a fully mixed approach is applied, in which the heat flux vector is incorporated as an additional unknown as well. Since the convective term in the heat equation forces both the velocity and the temperature to live in H^1 instead of L^2 as usual, we proceed as for the Boussinesq model in [8, 9, 10] and augment the variational formulation with suitable Galerkin type expressions arising from the constitutive and equilibrium equations, the relation defining the strain and vorticity tensors, and the Dirichlet boundary condition on the temperature. The resulting augmented scheme is then written equivalently as a fixed-point equation, so that the well-known Schauder and Banach theorems, combined with the Lax–Milgram theorem and certain regularity assumptions, are applied to prove the unique solvability of the continuous system. As for the associated Galerkin scheme, whose solvability is established similarly to the continuous case by using the Brouwer fixed-point and Lax–Milgram theorems, we employ Raviart–Thomas approximations of order k for the stress tensor and the heat flux vector, continuous piecewise polynomials of order $\leq k + 1$ for velocity and temperature, and piecewise polynomials of order $\leq k$ for the strain tensor and the vorticity. Optimal a priori error estimates were also derived.

Now, it is well known that under the eventual presence of singularities or high gradients of the solution, most of the standard Galerkin procedures such as finite element and mixed finite element methods inevitably lose accuracy, and hence one usually tries to recover it by applying an adaptive algorithm based on a posteriori error estimates. For example, residual-based a posteriori error analyses for the aforementioned Boussinesq model have been developed in [11] and [12] for the associated mixed-primal and fully-mixed formulations, respectively. In fact, standard arguments relying on duality techniques, suitable decompositions and classical approximation properties, are combined there with corresponding small data assumptions to derive the reliability of the estimators. In turn, inverse inequalities and the usual localisation technique based on bubble functions are employed in both works to prove the corresponding efficiency estimates. On the other hand, and concerning isothermal viscoelastic flows, not much has been done and we just refer to [17, 29, 30] for the steady-state case and [19, 20] for the time dependent case, where different contributions addressing this interesting issue can be found. In particular, a fully local a posteriori error estimator for a simplified Oldroyd-B model without convective terms in a convex polygonal domain was obtained in [30]. The main unknowns are given by the velocity, the extra-stress and the pressure of the fluid, whereas continuous piecewise linear finite elements together with a Galerkin Least Square (GLS) approach are used for the associated discrete scheme. In turn, a fully local residual-based a posteriori error estimator for the velocity-pressure-stress formulation of a more general model, namely the Giesekus and Oldroyd-B type differential constitutive laws in 2D and 3D, was derived in [17]. In this case, the discrete spaces employed are the Hood–Taylor pair for the velocity and the pressure, and continuous piecewise linear elements for the viscoelastic stress component. Furthermore, and up to the authors’ knowledge, the first work dealing with high gradients of the solution for the non-isothermal Oldroyd–Stokes problem is [14]. An optimal control technique is proposed and analysed there for a four-to-one contraction domain, where a vortex is generated near the corner region of the contraction. However, we remark that this work does not consider an adaptive algorithm.

According to the above discussion, and in order to complement the study started in [6] for the non-isothermal Oldroyd–Stokes problem, in this paper we proceed similarly to [1, 11, 12, 25], and develop two reliable and efficient residual-based a posteriori error estimators for the augmented-mixed finite element method studied in [6]. This means that our analysis begins by applying the uniform ellipticity of the bilinear form defining the continuous formulation. Next, we apply suitable Helmholtz decompositions, local approximation properties of the Clément and Raviart–Thomas interpolants, and known estimates from [23, 24], to prove the reliability of a residual-based estimator. In turn, the

efficiency estimate is consequence of standard arguments such as inverse inequalities, the localization technique based on bubble functions, and other known results to be specified later on in Section 3.4. Alternative, a second reliable and efficient residual-based a posteriori error estimator not making use of any Helmholtz decomposition is also proposed.

The rest of this work is organised as follows. The remainder of this section introduces some standard notations and functional spaces. In Section 2 we recall from [6, Section 2] the model problem and its continuous and discrete augmented fully-mixed variational formulations. Next, in Section 3 we consider the 2D case, introduce two a posteriori error indicators, and assuming small data and certain regularity assumptions, we derive the corresponding theoretical bounds yielding reliability and efficiency of each estimator. The analysis and results from Section 3 are then extended to the 3D case in Section 4. Finally, some numerical results illustrating the good performance and good effectivity indexes of both error estimators under diverse scenarios in 2D and 3D, and confirming the satisfactory behaviour of the corresponding adaptive refinement strategies, are presented in Section 5.

Preliminary notations

Let $\Omega \subseteq \mathbb{R}^n$, $n \in \{2, 3\}$, denote a bounded domain with Lipschitz boundary $\Gamma = \bar{\Gamma}_D \cup \bar{\Gamma}_N$, with $\Gamma_D \cap \Gamma_N = \emptyset$ and $|\Gamma_D|, |\Gamma_N| > 0$, and denote by \mathbf{n} the outward unit normal vector on Γ . For $s \geq 0$ and $p \in [1, +\infty]$, we define by $L^p(\Omega)$ and $W^{s,p}(\Omega)$ the usual Lebesgue and Sobolev spaces endowed with the norms $\|\cdot\|_{L^p(\Omega)}$ and $\|\cdot\|_{W^{s,p}(\Omega)}$, respectively. Note that $W^{0,p}(\Omega) = L^p(\Omega)$. If $p = 2$, we write $H^s(\Omega)$ in place of $W^{s,2}(\Omega)$, and denote the corresponding Lebesgue and Sobolev norms by $\|\cdot\|_{0,\Omega}$ and $\|\cdot\|_{s,\Omega}$, respectively, and the seminorm by $|\cdot|_{s,\Omega}$. By \mathbf{M} and \mathbb{M} we will denote the corresponding vectorial and tensorial counterparts of the generic scalar functional space M , and $\|\cdot\|$, with no subscripts, will stand for the natural norm of either an element or an operator in any product functional space. In turn, for any vector field $\mathbf{v} = (v_i)_{i=1,n}$, we set the gradient, and divergence operator, as

$$\nabla \mathbf{v} := \left(\frac{\partial v_i}{\partial x_j} \right)_{i,j=1,n} \quad \text{and} \quad \operatorname{div} \mathbf{v} := \sum_{j=1}^n \frac{\partial v_j}{\partial x_j}.$$

Furthermore, for any tensor fields $\boldsymbol{\tau} = (\tau_{ij})_{i,j=1,n}$ and $\boldsymbol{\zeta} = (\zeta_{ij})_{i,j=1,n}$, we let $\mathbf{div} \boldsymbol{\tau}$ be the divergence operator div acting along the rows of $\boldsymbol{\tau}$, and define the transpose, the trace, the tensor inner product, and the deviatoric tensor, respectively, as

$$\boldsymbol{\tau}^t := (\tau_{ji})_{i,j=1,n}, \quad \operatorname{tr}(\boldsymbol{\tau}) := \sum_{i=1}^n \tau_{ii}, \quad \boldsymbol{\tau} : \boldsymbol{\zeta} := \sum_{i,j=1}^n \tau_{ij} \zeta_{ij}, \quad \text{and} \quad \boldsymbol{\tau}^d := \boldsymbol{\tau} - \frac{1}{n} \operatorname{tr}(\boldsymbol{\tau}) \mathbb{I},$$

where \mathbb{I} is the identity matrix in $\mathbb{R}^{n \times n}$. Additionally, we define the following tensorial and vectorial functional spaces (see [6, Section 2.2] for details):

$$\begin{aligned} \mathbb{H}_0(\mathbf{div}; \Omega) &:= \left\{ \boldsymbol{\tau} \in \mathbb{H}(\mathbf{div}; \Omega) : \int_{\Omega} \operatorname{tr} \boldsymbol{\tau} = 0 \right\}, \\ \mathbb{L}_{\operatorname{tr}}^2(\Omega) &:= \left\{ \mathbf{r} \in \mathbb{L}^2(\Omega) : \mathbf{r}^t = \mathbf{r} \quad \text{and} \quad \operatorname{tr} \mathbf{r} = 0 \right\}, \\ \mathbb{L}_{\operatorname{skew}}^2(\Omega) &:= \left\{ \boldsymbol{\eta} \in \mathbb{L}^2(\Omega) : \boldsymbol{\eta}^t = -\boldsymbol{\eta} \right\}, \end{aligned} \tag{1.1}$$

and

$$\mathbf{H}_{\Gamma_N}(\operatorname{div}; \Omega) := \left\{ \mathbf{q} \in \mathbf{H}(\operatorname{div}; \Omega) : \mathbf{q} \cdot \mathbf{n} = 0 \quad \text{on} \quad \Gamma_N \right\}, \tag{1.2}$$

respectively. Furthermore, given an integer $k \geq 0$ and a set $S \subseteq \mathbb{R}^n$, $\mathbf{P}_k(S)$ denotes the space of polynomial functions on S of degree $\leq k$. In addition, and coherently with previous notations, we set $\mathbf{P}_k(S) := [\mathbf{P}_k(S)]^n$ and $\mathbb{P}_k(S) := [\mathbf{P}_k(S)]^{n \times n}$. Finally, we end this section by mentioning that, throughout the rest of the paper, we employ $\mathbf{0}$ to denote a generic null vector (or tensor), and use C and c , with or without subscripts, bars, tildes or hats, to denote generic constants independent of the discretization parameters, which may take different values at different places.

2 The non-isothermal Oldroyd–Stokes problem

In this section we recall from [6] the non-isothermal Oldroyd–Stokes model, its fully-mixed variational formulation, the associated Galerkin scheme, and the main results concerning the corresponding solvability analysis.

2.1 The model problem

The non-isothermal Oldroyd–Stokes problem consists of a system of equations where the Stokes equation for the Oldroyd viscoelastic model introduced in [2], is coupled with the heat equation through a convective term and the viscosity of the fluid (cf. [13, 18]). More precisely, given a body force \mathbf{f} , and a heat source g , the aforementioned system of equations is given by

$$\begin{aligned} \boldsymbol{\sigma}_P - 2\mu_P(\theta)\mathbf{e}(\mathbf{u}) &= \mathbf{0} \quad \text{in } \Omega, & -\mathbf{div}(\boldsymbol{\sigma}_P + 2\epsilon\mu_N(\theta)\mathbf{e}(\mathbf{u})) + \nabla p &= \mathbf{f} \quad \text{in } \Omega, \\ \mathbf{div} \mathbf{u} &= 0 \quad \text{in } \Omega, & -\mathbf{div}(\kappa\nabla\theta) + \mathbf{u} \cdot \nabla\theta &= g \quad \text{in } \Omega, \\ \mathbf{u} &= \mathbf{0} \quad \text{on } \Gamma, & \theta &= \theta_D \quad \text{on } \Gamma_D, & \kappa\nabla\theta \cdot \mathbf{n} &= 0 \quad \text{on } \Gamma_N \quad \text{and} \quad \int_{\Omega} p = 0, \end{aligned} \tag{2.1}$$

where the unknowns are the polymeric part of the extra-stress tensor $\boldsymbol{\sigma}_P$, the velocity \mathbf{u} , the pressure p , and the temperature θ of a fluid occupying the region Ω . In addition, $\mathbf{e}(\mathbf{u}) := \frac{1}{2}\{\nabla\mathbf{u} + (\nabla\mathbf{u})^t\}$ stands for the strain tensor of small deformations, κ is the thermal conductivity coefficient, μ_P and μ_N are the polymeric and solvent (or newtonian) viscosities, respectively, which are given by the following Arrhenius relationship:

$$\mu_P(\theta) = a_1 \exp\left(\frac{b_1}{\theta}\right), \quad \mu_N(\theta) = a_2 \exp\left(\frac{b_2}{\theta}\right), \tag{2.2}$$

where the coefficients a_1, b_1, a_2 , and b_2 are defined so that

$$0 < \mu_P(s) \leq 1, \quad 0 < \mu_N(s) \leq 1 \quad \forall s \geq 0. \tag{2.3}$$

Furthermore, we assume that both the polymeric and solvent viscosities are Lipschitz continuous and bounded from above and from below, that is,

$$|\mu_P(s) - \mu_P(t)| \leq L_{\mu_P}|s - t|, \quad |\mu_N(s) - \mu_N(t)| \leq L_{\mu_N}|s - t| \quad \forall s, t \geq 0, \tag{2.4}$$

and

$$\mu_{1,P} \leq \mu_P(s) \leq \mu_{2,P}, \quad \mu_{1,N} \leq \mu_N(s) \leq \mu_{2,N} \quad \forall s \geq 0. \tag{2.5}$$

Note that a small real parameter $\epsilon > 0$ on the second equation of (2.1) is introduced to make the effect of the solvent viscosity much smaller than that of the polymeric part.

Now, in order to derive our mixed approach (see [6, Section 2.1] for details), we begin by introducing the strain tensor as an additional unknown $\mathbf{t} := \mathbf{e}(\mathbf{u})$, whence the polymeric and solvent parts of the extra-stress tensor can be written, respectively, as

$$\boldsymbol{\sigma}_P = 2\mu_P(\theta)\mathbf{t} \quad \text{and} \quad \boldsymbol{\sigma}_N = 2\epsilon\mu_N(\theta)\mathbf{t} \quad \text{in } \Omega. \quad (2.6)$$

Next, defining the dimensionless effective viscosity as in [18], that is

$$\mu(\theta) := 2\mu_P(\theta) + 2\epsilon\mu_N(\theta), \quad (2.7)$$

and adopting the approach from [24] and [18] (see also [5, 8, 10]), we include as auxiliary variables the vorticity tensor $\boldsymbol{\rho}$, the stress tensor $\boldsymbol{\sigma}$, and the heat-flux vector \mathbf{p} , respectively, by

$$\boldsymbol{\rho} := \nabla\mathbf{u} - \mathbf{e}(\mathbf{u}), \quad \boldsymbol{\sigma} := \mu(\theta)\mathbf{t} - p\mathbb{I}, \quad \text{and} \quad \mathbf{p} := \kappa\nabla\theta - \theta\mathbf{u} \quad \text{in } \Omega.$$

In this way, utilising the incompressibility condition $\operatorname{div} \mathbf{u} = \operatorname{tr}(\mathbf{e}(\mathbf{u})) = 0$ in Ω and the homogeneous Dirichlet boundary condition $\mathbf{u} = \mathbf{0}$ on Γ , the equations in (2.1) can be rewritten, equivalently, as

$$\begin{aligned} \mathbf{t} + \boldsymbol{\rho} &= \nabla\mathbf{u} \quad \text{in } \Omega, & \boldsymbol{\sigma}^d &= \mu(\theta)\mathbf{t} \quad \text{in } \Omega, & -\operatorname{div} \boldsymbol{\sigma} &= \mathbf{f} \quad \text{in } \Omega, \\ p &= -\frac{1}{n}\operatorname{tr} \boldsymbol{\sigma} \quad \text{in } \Omega, & \kappa^{-1}\mathbf{p} + \kappa^{-1}\theta\mathbf{u} &= \nabla\theta \quad \text{in } \Omega, & -\operatorname{div} \mathbf{p} &= g \quad \text{in } \Omega, \\ \mathbf{u} &= \mathbf{0} \quad \text{on } \Gamma, & \theta &= \theta_D \quad \text{on } \Gamma_D, & \mathbf{p} \cdot \mathbf{n} &= 0 \quad \text{on } \Gamma_N \quad \text{and} \quad \int_{\Omega} \operatorname{tr} \boldsymbol{\sigma} = 0. \end{aligned} \quad (2.8)$$

Note that the fourth equation in (2.8) allows us to eliminate the pressure p from the system and compute it as a simple post-process of $\boldsymbol{\sigma}$. In addition, it easy to see from (2.4) and (2.5) that the fluid viscosity μ (cf. (2.7)) is Lipschitz continuous and bounded from above and from below, that is, there exist constants $L_\mu > 0$ and $\mu_1, \mu_2 > 0$, such that

$$|\mu(s) - \mu(t)| \leq L_\mu |s - t| \quad \forall s, t \geq 0, \quad (2.9)$$

and

$$\mu_1 \leq \mu(s) \leq \mu_2 \quad \forall s \geq 0. \quad (2.10)$$

We end this section emphasizing from (2.6) that we can recover the polymeric and solvent parts of the extra-stress tensor as a simple post-process of θ and \mathbf{t} , whereas from the fourth equation of (2.8) we can compute the pressure in terms of $\boldsymbol{\sigma}$ conserving the same rate of convergence of the solution as we show theoretical and numerically in [6, Lemma 4.14 and Section 5], respectively. However, for the sake of simplicity and physical interest, in Section 5 we will focus only on the formulae suggested for the polymeric part of the extra-stress tensor and the pressure.

2.2 The fully-mixed variational formulation

In this section we recall from [6, Section 2.2] the weak formulation of the coupled problem given by (2.8). To this end, let us first group appropriately some of the unknowns and spaces as follows:

$$\underline{\mathbf{t}} := (\mathbf{t}, \boldsymbol{\sigma}, \boldsymbol{\rho}) \in \mathbb{H} := \mathbb{L}_{\operatorname{tr}}^2(\Omega) \times \mathbb{H}_0(\operatorname{div}; \Omega) \times \mathbb{L}_{\operatorname{skew}}^2(\Omega),$$

where \mathbb{H} is endowed with the norm

$$\|\underline{\mathbf{r}}\|_{\mathbb{H}}^2 := \|\mathbf{r}\|_{0,\Omega}^2 + \|\boldsymbol{\tau}\|_{\operatorname{div};\Omega}^2 + \|\boldsymbol{\eta}\|_{0,\Omega}^2 \quad \forall \underline{\mathbf{r}} := (\mathbf{r}, \boldsymbol{\tau}, \boldsymbol{\eta}) \in \mathbb{H}.$$

Hence, the augmented fully-mixed variational formulation for the non-isothermal Oldroyd–Stokes problem reads: Find $(\underline{\mathbf{t}}, \mathbf{u}, \mathbf{p}, \theta) \in \mathbb{H} \times \mathbf{H}_0^1(\Omega) \times \mathbf{H}_{\Gamma_N}(\text{div}; \Omega) \times H^1(\Omega)$ such that

$$\begin{aligned} \mathbf{A}_\theta((\underline{\mathbf{t}}, \mathbf{u}), (\underline{\mathbf{r}}, \mathbf{v})) &= \mathbf{F}(\underline{\mathbf{r}}, \mathbf{v}) \quad \forall (\underline{\mathbf{r}}, \mathbf{v}) \in \mathbb{H} \times \mathbf{H}_0^1(\Omega), \\ \tilde{\mathbf{A}}((\mathbf{p}, \theta), (\mathbf{q}, \psi)) + \tilde{\mathbf{B}}_{\mathbf{u}}((\mathbf{p}, \theta), (\mathbf{q}, \psi)) &= \tilde{\mathbf{F}}(\mathbf{q}, \psi) \quad \forall (\mathbf{q}, \psi) \in \mathbf{H}_{\Gamma_N}(\text{div}; \Omega) \times H^1(\Omega), \end{aligned} \quad (2.11)$$

where, given $(\phi, \mathbf{w}) \in H^1(\Omega) \times \mathbf{H}_0^1(\Omega)$, \mathbf{A}_ϕ , $\tilde{\mathbf{A}}$, and $\tilde{\mathbf{B}}_{\mathbf{w}}$ are the bilinear forms defined, respectively, as

$$\begin{aligned} \mathbf{A}_\phi((\underline{\mathbf{t}}, \mathbf{u}), (\underline{\mathbf{r}}, \mathbf{v})) &:= \int_{\Omega} \mu(\phi) \underline{\mathbf{t}} : \{ \underline{\mathbf{r}} - \kappa_1 \boldsymbol{\tau}^{\text{d}} \} + \int_{\Omega} \boldsymbol{\sigma}^{\text{d}} : \{ \kappa_1 \boldsymbol{\tau}^{\text{d}} - \underline{\mathbf{r}} \} + \int_{\Omega} \underline{\mathbf{t}} : \boldsymbol{\tau}^{\text{d}} \\ &+ \int_{\Omega} \{ \mathbf{u} + \kappa_2 \text{div } \boldsymbol{\sigma} \} \cdot \text{div } \boldsymbol{\tau} - \int_{\Omega} \mathbf{v} \cdot \text{div } \boldsymbol{\sigma} + \int_{\Omega} \boldsymbol{\rho} : \boldsymbol{\tau} - \int_{\Omega} \boldsymbol{\sigma} : \boldsymbol{\eta} \\ &+ \kappa_3 \int_{\Omega} \{ \mathbf{e}(\mathbf{u}) - \underline{\mathbf{t}} \} : \mathbf{e}(\mathbf{v}) + \kappa_4 \int_{\Omega} \left(\boldsymbol{\rho} - \{ \nabla \mathbf{u} - \mathbf{e}(\mathbf{u}) \} \right) : \boldsymbol{\eta}, \end{aligned} \quad (2.12)$$

$$\begin{aligned} \tilde{\mathbf{A}}((\mathbf{p}, \theta), (\mathbf{q}, \psi)) &:= \kappa^{-1} \int_{\Omega} \mathbf{p} \cdot \{ \mathbf{q} - \kappa_5 \nabla \psi \} + \int_{\Omega} \{ \theta + \kappa_6 \text{div } \mathbf{p} \} \text{div } \mathbf{q} - \int_{\Omega} \psi \text{div } \mathbf{p} \\ &+ \kappa_5 \int_{\Omega} \nabla \theta \cdot \nabla \psi + \kappa_7 \int_{\Gamma_D} \theta \psi, \end{aligned} \quad (2.13)$$

and

$$\tilde{\mathbf{B}}_{\mathbf{w}}((\mathbf{p}, \theta), (\mathbf{q}, \psi)) := \kappa^{-1} \int_{\Omega} \theta \mathbf{w} \cdot \{ \mathbf{q} - \kappa_5 \nabla \psi \}, \quad (2.14)$$

for all $(\underline{\mathbf{t}}, \mathbf{u}), (\underline{\mathbf{r}}, \mathbf{v}) \in \mathbb{H} \times \mathbf{H}_0^1(\Omega)$ and for all $(\mathbf{p}, \theta), (\mathbf{q}, \psi) \in \mathbf{H}_{\Gamma_N}(\text{div}; \Omega) \times H^1(\Omega)$. In turn, \mathbf{F} and $\tilde{\mathbf{F}}$ are the bounded linear functionals given by

$$\mathbf{F}(\underline{\mathbf{r}}, \mathbf{v}) := \int_{\Omega} \mathbf{f} \cdot \{ \mathbf{v} - \kappa_2 \text{div } \boldsymbol{\tau} \}, \quad (2.15)$$

for all $(\underline{\mathbf{r}}, \mathbf{v}) \in \mathbb{H} \times \mathbf{H}_0^1(\Omega)$ and

$$\tilde{\mathbf{F}}(\mathbf{q}, \psi) := \langle \mathbf{q} \cdot \mathbf{n}, \theta_D \rangle_{\Gamma_D} + \int_{\Omega} g \{ \psi - \kappa_6 \text{div } \mathbf{q} \} + \kappa_7 \int_{\Gamma_D} \theta_D \psi, \quad (2.16)$$

for all $(\mathbf{q}, \psi) \in \mathbf{H}_{\Gamma_N}(\text{div}; \Omega) \times H^1(\Omega)$. Notice that $\kappa_i, i \in \{1, \dots, 7\}$, are positive parameters to be specified next in Theorem 2.1. Indeed, the following result taken from [6] establishes the well-posedness of (2.11).

Theorem 2.1 *Assume that*

$$\kappa_1 \in \left(0, \frac{2\delta_1 \mu_1}{\mu_2} \right), \quad \kappa_3 \in \left(0, 2\delta_2 \left(\mu_1 - \frac{\kappa_1 \mu_2}{2\delta_1} \right) \right), \quad \kappa_4 \in \left(0, 2\delta_3 \kappa_3 \left(1 - \frac{\delta_2}{2} \right) \right), \quad \kappa_5 \in (0, 2\tilde{\delta}),$$

and $\kappa_2, \kappa_6, \kappa_7 > 0$, with $\delta_1 \in \left(0, \frac{2}{\mu_2} \right)$, $\delta_2, \delta_3 \in (0, 2)$, and $\tilde{\delta} \in (0, 2\kappa)$. Let

$$\mathcal{W} := \left\{ \phi \in H^1(\Omega) : \|\phi\|_{1,\Omega} \leq c_{\tilde{\mathbf{S}}} \left\{ \|g\|_{0,\Omega} + \|\theta_D\|_{0,\Gamma_D} + \|\theta_D\|_{1/2,\Gamma_D} \right\} \right\},$$

and assume that the datum \mathbf{f} satisfy

$$c_{\mathbf{S}} \|\mathbf{f}\|_{0,\Omega} \leq \frac{\tilde{\alpha}(\Omega)}{2\kappa^{-1}(1 + \kappa_5^2)^{1/2} c(\Omega)}, \quad (2.17)$$

where $c(\Omega)$ is the constant in [6, eq. (2.15)], $\tilde{\alpha}(\Omega)$ is the ellipticity constant of the bilinear form $\tilde{\mathbf{A}}$ (cf. [6, eq. (3.17)]), and $c_{\mathbf{S}}$ and $c_{\tilde{\mathbf{S}}}$ are the positive constants, independent of the data, provided by [6, Lemmas 3.1 and 3.2], respectively. Then the augmented fully-mixed problem (2.11) has at least one solution $(\mathbf{t}, \mathbf{u}, \mathbf{p}, \theta) \in \mathbb{H} \times \mathbf{H}_0^1(\Omega) \times \mathbf{H}_{\Gamma_N}(\text{div}; \Omega) \times \mathbf{H}^1(\Omega)$ with $\theta \in \mathcal{W}$, and there holds

$$\|(\mathbf{t}, \mathbf{u})\| \leq c_{\mathbf{S}} \|\mathbf{f}\|_{0,\Omega} \quad \text{and} \quad \|(\mathbf{p}, \theta)\| \leq c_{\tilde{\mathbf{S}}} \left\{ \|g\|_{0,\Omega} + \|\theta_D\|_{0,\Gamma_D} + \|\theta_D\|_{1/2,\Gamma_D} \right\}. \quad (2.18)$$

Moreover, if the data \mathbf{f} , g and θ_D are sufficiently small so that, with the constants $C_{\mathbf{S}}$, $C_{\tilde{\mathbf{S}}}$ and $\hat{C}_{\mathbf{S}}$ from [6, Lemmas 3.4 and 3.5, and eq. (3.22)], respectively, and denoting by \tilde{C}_{δ} the boundedness constant of the continuous injection of $\mathbf{H}^1(\Omega)$ into $L^{n/\delta}(\Omega)$, with $\delta \in (0, 1)$ (when $n = 2$) or $\delta \in (1/2, 1)$ (when $n = 3$), there holds

$$\tilde{C}_{\delta} \hat{C}_{\mathbf{S}} C_{\mathbf{S}} C_{\tilde{\mathbf{S}}} c_{\tilde{\mathbf{S}}} \left\{ \|g\|_{0,\Omega} + \|\theta_D\|_{0,\Gamma_D} + \|\theta_D\|_{1/2,\Gamma_D} \right\} \|\mathbf{f}\|_{\delta,\Omega} < 1. \quad (2.19)$$

Then the solution θ is unique in \mathcal{W} .

Proof. See [6, Theorem 3.8] for details. \square

2.3 The fully-mixed finite element method

Let \mathcal{T}_h be a regular triangulation of Ω made up of triangles T (when $n = 2$) or tetrahedra T (when $n = 3$) of diameter h_T , and define the meshsize $h := \max \{h_T : T \in \mathcal{T}_h\}$. Then, given an integer $k \geq 0$, we set for each $T \in \mathcal{T}_h$ the local Raviart–Thomas space of order k as

$$\mathbf{RT}_k(T) := \mathbf{P}_k(T) \oplus \mathbf{P}_k(T)\mathbf{x},$$

where $\mathbf{x} := (x_1, \dots, x_n)^{\mathbf{t}}$ is a generic vector of \mathbb{R}^n . Then, we introduce the finite element subspaces approximating the unknowns $\mathbf{t}, \boldsymbol{\sigma}, \boldsymbol{\rho}, \mathbf{u}, \mathbf{p}$ and θ as follows

$$\begin{aligned} \mathbb{H}_h^{\mathbf{t}} &:= \left\{ \mathbf{r}_h \in \mathbb{L}_{\text{tr}}^2(\Omega) : \mathbf{r}_h|_T \in \mathbf{P}_k(T) \quad \forall T \in \mathcal{T}_h \right\}, \\ \mathbb{H}_h^{\boldsymbol{\sigma}} &:= \left\{ \boldsymbol{\tau}_h \in \mathbb{H}_0(\text{div}; \Omega) : \mathbf{c}^{\mathbf{t}} \boldsymbol{\tau}_h|_T \in \mathbf{RT}_k(T) \quad \forall \mathbf{c} \in \mathbb{R}^n \quad \forall T \in \mathcal{T}_h \right\}, \\ \mathbb{H}_h^{\boldsymbol{\rho}} &:= \left\{ \boldsymbol{\eta}_h \in \mathbb{L}_{\text{skew}}^2(\Omega) : \boldsymbol{\eta}_h|_T \in \mathbf{P}_k(T) \quad \forall T \in \mathcal{T}_h \right\}, \\ \mathbf{H}_h^{\mathbf{u}} &:= \left\{ \mathbf{v}_h \in \mathbf{C}(\bar{\Omega}) : \mathbf{v}_h|_T \in \mathbf{P}_{k+1}(T) \quad \forall T \in \mathcal{T}_h, \quad \mathbf{v}_h = 0 \text{ on } \Gamma \right\}, \\ \mathbf{H}_h^{\mathbf{p}} &:= \left\{ \mathbf{q}_h \in \mathbf{H}_{\Gamma_N}(\text{div}; \Omega) : \mathbf{q}_h|_T \in \mathbf{RT}_k(T) \quad \forall T \in \mathcal{T}_h \right\}, \\ \mathbf{H}_h^{\theta} &:= \left\{ \psi_h \in C(\bar{\Omega}) : \psi_h|_T \in \mathbf{P}_{k+1}(T) \quad \forall T \in \mathcal{T}_h \right\}. \end{aligned} \quad (2.20)$$

In this way, by defining $\mathbf{t}_h := (\mathbf{t}_h, \boldsymbol{\sigma}_h, \boldsymbol{\rho}_h)$, $\mathbf{r}_h := (\mathbf{r}_h, \boldsymbol{\tau}_h, \boldsymbol{\eta}_h) \in \mathbb{H}_h := \mathbb{H}_h^{\mathbf{t}} \times \mathbb{H}_h^{\boldsymbol{\sigma}} \times \mathbb{H}_h^{\boldsymbol{\rho}}$, the Galerkin scheme of (2.11) reads: Find $(\mathbf{t}_h, \mathbf{u}_h, \mathbf{p}_h, \theta_h) \in \mathbb{H}_h \times \mathbf{H}_h^{\mathbf{u}} \times \mathbf{H}_h^{\mathbf{p}} \times \mathbf{H}_h^{\theta}$ such that

$$\begin{aligned} \mathbf{A}_{\theta_h}((\mathbf{t}_h, \mathbf{u}_h), (\mathbf{r}_h, \mathbf{v}_h)) &= \mathbf{F}(\mathbf{r}_h, \mathbf{v}_h) \quad \forall (\mathbf{r}_h, \mathbf{v}_h) \in \mathbb{H}_h \times \mathbf{H}_h^{\mathbf{u}}, \\ \tilde{\mathbf{A}}((\mathbf{p}_h, \theta_h), (\mathbf{q}_h, \psi_h)) + \tilde{\mathbf{B}}_{\mathbf{u}_h}((\mathbf{p}_h, \theta_h), (\mathbf{q}_h, \psi_h)) &= \tilde{\mathbf{F}}(\mathbf{q}_h, \psi_h) \quad \forall (\mathbf{q}_h, \psi_h) \in \mathbf{H}_h^{\mathbf{p}} \times \mathbf{H}_h^{\theta}. \end{aligned} \quad (2.21)$$

The following theorem, also taken from [6], provides the well-posedness of (2.21), the associated C ea estimate, and the corresponding theoretical rate of convergence.

Theorem 2.2 Assume that the conditions on κ_i , $i \in \{1, \dots, 7\}$, required by Theorem 2.1, hold. Let

$$\mathcal{W}_h := \left\{ \phi_h \in \mathbf{H}_h^\theta : \|\phi_h\|_{1,\Omega} \leq c_{\mathfrak{S}} \left\{ \|g\|_{0,\Omega} + \|\theta_D\|_{0,\Gamma_D} + \|\theta_D\|_{1/2,\Gamma_D} \right\} \right\},$$

and assume that the datum \mathbf{f} satisfy (2.17). Then the Galerkin scheme (2.21) has at least one solution $(\underline{\mathbf{t}}_h, \mathbf{u}_h, \mathbf{p}_h, \theta_h) \in \mathbb{H}_h \times \mathbf{H}_h^{\mathbf{u}} \times \mathbf{H}_h^{\mathbf{p}} \times \mathbf{H}_h^\theta$ with $\theta_h \in \mathcal{W}_h$, and there holds

$$\|(\underline{\mathbf{t}}_h, \mathbf{u}_h)\| \leq c_{\mathfrak{S}} \|\mathbf{f}\|_{0,\Omega} \quad \text{and} \quad \|(\mathbf{p}_h, \theta_h)\| \leq c_{\mathfrak{S}} \left\{ \|g\|_{0,\Omega} + \|\theta_D\|_{0,\Gamma_D} + \|\theta_D\|_{1/2,\Gamma_D} \right\}. \quad (2.22)$$

In addition, there exists $C_1 > 0$, independent of h , such that

$$\|(\underline{\mathbf{t}}, \mathbf{u}, \mathbf{p}, \theta) - (\underline{\mathbf{t}}_h, \mathbf{u}_h, \mathbf{p}_h, \theta_h)\| \leq C_1 \left\{ \text{dist} \left((\underline{\mathbf{t}}, \mathbf{u}), \mathbb{H}_h \times \mathbf{H}_h^{\mathbf{u}} \right) + \text{dist} \left((\mathbf{p}, \theta), \mathbf{H}_h^{\mathbf{p}} \times \mathbf{H}_h^\theta \right) \right\}.$$

Assume further that there exists $s > 0$ such that $\mathbf{t} \in \mathbb{H}^s(\Omega)$, $\boldsymbol{\sigma} \in \mathbb{H}^s(\Omega)$, $\text{div } \boldsymbol{\sigma} \in \mathbf{H}^s(\Omega)$, $\boldsymbol{\rho} \in \mathbb{H}^s(\Omega)$, $\mathbf{u} \in \mathbf{H}^{s+1}(\Omega)$, $\mathbf{p} \in \mathbf{H}^s(\Omega)$, $\text{div } \mathbf{p} \in \mathbf{H}^s(\Omega)$, and $\theta \in \mathbf{H}^{s+1}(\Omega)$, and that the finite element subspaces are defined by (2.20). Then, there exist $C_2 > 0$, independent of h , such that

$$\begin{aligned} \|(\underline{\mathbf{t}}, \mathbf{u}, \mathbf{p}, \theta) - (\underline{\mathbf{t}}_h, \mathbf{u}_h, \mathbf{p}_h, \theta_h)\| &\leq C_2 h^{\min\{s, k+1\}} \left\{ \|\mathbf{t}\|_{s,\Omega} + \|\boldsymbol{\sigma}\|_{s,\Omega} + \|\text{div } \boldsymbol{\sigma}\|_{s,\Omega} + \|\boldsymbol{\rho}\|_{s,\Omega} \right. \\ &\quad \left. + \|\mathbf{u}\|_{s+1,\Omega} + \|\mathbf{p}\|_{s,\Omega} + \|\text{div } \mathbf{p}\|_{s,\Omega} + \|\theta\|_{s+1,\Omega} \right\}. \end{aligned}$$

Proof. We refer the reader to [6, Theorems 4.7, 4.11, and 4.13] for details. \square

3 A posteriori error analysis: the 2D-case

In this section we proceed analogously to [25, Section 3] and derive two reliable and efficient residual based a posteriori error estimators for the two-dimensional version of (2.21). The corresponding a posteriori error analysis for the 3D case, which follows from minor modifications of the one to be presented next, will be addressed in Section 4.

3.1 Preliminaries

We start by introducing a few useful notations for describing local information on elements and edges. Let \mathcal{E}_h be the set of all edges of \mathcal{T}_h , and $\mathcal{E}(T)$ denotes the set of edges of a given $T \in \mathcal{T}_h$. Then $\mathcal{E}_h = \mathcal{E}_h(\Omega) \cup \mathcal{E}_h(\Gamma_D) \cup \mathcal{E}_h(\Gamma_N)$, where $\mathcal{E}_h(\Omega) := \{e \in \mathcal{E}_h : e \subseteq \Omega\}$, $\mathcal{E}_h(\Gamma_D) := \{e \in \mathcal{E}_h : e \subseteq \Gamma_D\}$, and $\mathcal{E}_h(\Gamma_N) := \{e \in \mathcal{E}_h : e \subseteq \Gamma_N\}$. Moreover, h_e stands for the length of a given edge e . Also for each edge $e \in \mathcal{E}_h$ we fix a unit normal vector $\mathbf{n}_e := (n_1, n_2)^t$, and let $\mathbf{s}_e := (-n_2, n_1)^t$ be the corresponding fixed unit tangential vector along e . However, when no confusion arises, we simply write \mathbf{n} and \mathbf{s} instead of \mathbf{n}_e and \mathbf{s}_e , respectively. Now, let $\mathbf{v} \in \mathbf{L}^2(\Omega)$ such that $\mathbf{v}|_T \in \mathbf{C}(T)$ on each $T \in \mathcal{T}_h$. Then, given $T \in \mathcal{T}_h$ and $e \in \mathcal{E}(T) \cap \mathcal{E}_h(\Omega)$, we denote by $\llbracket \mathbf{v} \cdot \mathbf{s} \rrbracket$ the tangential jump of \mathbf{v} across e , that is, $\llbracket \mathbf{v} \cdot \mathbf{s} \rrbracket := (\mathbf{v}|_T - \mathbf{v}|_{T'})|_e \cdot \mathbf{s}$, where T and T' are the triangles of \mathcal{T}_h having e as a common edge. Similar definitions hold for the tangential jumps of scalar and tensor fields $\phi \in L^2(\Omega)$ and $\boldsymbol{\tau} \in \mathbb{L}^2(\Omega)$, respectively, such that $\phi|_T \in C(T)$ and $\boldsymbol{\tau}|_T \in \mathbb{C}(T)$ on each $T \in \mathcal{T}_h$. In addition, given scalar, vector and matrix valued fields ϕ , $\mathbf{v} = (v_1, v_2)^t$ and $\boldsymbol{\tau} = (\tau_{i,j})_{1 \leq i,j \leq 2}$, respectively, we set

$$\begin{aligned} \text{curl}(\phi) &:= \begin{pmatrix} \frac{\partial \phi}{\partial x_2} \\ -\frac{\partial \phi}{\partial x_1} \end{pmatrix}, \quad \underline{\text{curl}}(\mathbf{v}) := \begin{pmatrix} \text{curl}(v_1)^t \\ \text{curl}(v_2)^t \end{pmatrix}, \\ \text{rot}(\mathbf{v}) &= \frac{\partial v_2}{\partial x_1} - \frac{\partial v_1}{\partial x_2}, \quad \text{and} \quad \text{rot}(\boldsymbol{\tau}) = \begin{pmatrix} \frac{\partial \tau_{12}}{\partial x_1} - \frac{\partial \tau_{11}}{\partial x_2}, \frac{\partial \tau_{22}}{\partial x_1} - \frac{\partial \tau_{21}}{\partial x_2} \end{pmatrix}^t, \end{aligned}$$

where the derivatives involved are taken in the distributional sense.

Let us now $\Pi_h : \mathbf{H}^1(\Omega) \rightarrow \mathbf{H}_h^{\mathbf{P}}$ (cf. (2.20)) be the Raviart–Thomas interpolation operator, which, according to its characterisation properties (see, e.g., [21, Section 3.4.1]), verifies

$$\operatorname{div}(\Pi_h \mathbf{v}) = \mathcal{P}_h(\operatorname{div} \mathbf{v}) \quad \forall \mathbf{v} \in \mathbf{H}^1(\Omega), \quad (3.1)$$

where \mathcal{P}_h is the $L^2(\Omega)$ -orthogonal projector onto the piecewise polynomials of degree $\leq k$. A tensor version of Π_h , say $\mathbf{\Pi}_h : \mathbb{H}^1(\Omega) \rightarrow \mathbb{H}_h^{\boldsymbol{\sigma}}$, which is defined row-wise by Π_h , and a vector version of \mathcal{P}_h , say \mathbf{P}_h , which is the $\mathbf{L}^2(\Omega)$ -orthogonal projector onto the piecewise polynomial vectors of degree $\leq k$, might also be required. The local approximation properties of Π_h (and hence of $\mathbf{\Pi}_h$) are established in what follows. For the corresponding proof we refer to [21, Lemmas 3.16 and 3.18] (see also [4]).

Lemma 3.1 *There exist constants $c_1, c_2 > 0$, independent of h , such that for all $\mathbf{v} \in \mathbf{H}^1(\Omega)$ there hold*

$$\|\mathbf{v} - \Pi_h \mathbf{v}\|_{0,T} \leq c_1 h_T \|\mathbf{v}\|_{1,T} \quad \forall T \in \mathcal{T}_h,$$

and

$$\|\mathbf{v} \cdot \mathbf{n} - \Pi_h \mathbf{v} \cdot \mathbf{n}\|_{0,e} \leq c_2 h_e^{1/2} \|\mathbf{v}\|_{1,T_e} \quad \forall e \in \mathcal{E}_h,$$

where T_e is a triangle of \mathcal{T}_h containing the edge e on its boundary.

In turn, let $I_h : \mathbf{H}^1(\Omega) \rightarrow \mathbf{H}_h^1(\Omega)$ be the Clément interpolation operator, where

$$\mathbf{H}_h^1(\Omega) := \left\{ v \in C(\overline{\Omega}) : v|_T \in \mathbf{P}_1(T) \quad \forall T \in \mathcal{T}_h \right\}.$$

The local approximation properties of this operator are established in the following lemma (see [7]).

Lemma 3.2 *There exist constants $c_3, c_4 > 0$, independent of h , such that for all $v \in \mathbf{H}^1(\Omega)$ there holds*

$$\|v - I_h v\|_{0,T} \leq c_3 h_T \|v\|_{1,\Delta(T)} \quad \forall T \in \mathcal{T}_h,$$

and

$$\|v - I_h v\|_{0,e} \leq c_4 h_e^{1/2} \|v\|_{1,\Delta(e)} \quad \forall e \in \mathcal{E}_h,$$

where

$$\Delta(T) := \cup \left\{ T' \in \mathcal{T}_h : T' \cap T \neq \emptyset \right\} \quad \text{and} \quad \Delta(e) := \cup \left\{ T' \in \mathcal{T}_h : T' \cap e \neq \emptyset \right\}.$$

In what follows, a vector version of I_h , say $\mathbf{I}_h : \mathbf{H}^1(\Omega) \rightarrow \mathbf{H}_h^1(\Omega)$, which is defined component-wise by I_h , will be needed as well. For the forthcoming analysis we will also utilise a couple of results providing stable Helmholtz decompositions for $\mathbb{H}_0(\mathbf{div}; \Omega)$ and $\mathbf{H}_{\Gamma_N}(\mathbf{div}; \Omega)$. In this regard, we remark in advance that the decomposition for $\mathbf{H}_{\Gamma_N}(\mathbf{div}; \Omega)$ will require the boundary Γ_N to lie in a “convex part” of Ω , which means that there exists a convex domain containing Ω , and whose boundary contains Γ_N . More precisely, we have the following lemma (cf. (1.1), (1.2)).

Lemma 3.3

(a) *For each $\boldsymbol{\tau} \in \mathbb{H}_0(\mathbf{div}; \Omega)$ there exist $\mathbf{z} \in \mathbf{H}^2(\Omega)$ and $\boldsymbol{\varphi} \in \mathbf{H}^1(\Omega)$ such that*

$$\boldsymbol{\tau} = \nabla \mathbf{z} + \mathbf{curl} \boldsymbol{\varphi} \quad \text{in } \Omega \quad \text{and} \quad \|\mathbf{z}\|_{2,\Omega} + \|\boldsymbol{\varphi}\|_{1,\Omega} \leq C \|\boldsymbol{\tau}\|_{\mathbf{div}; \Omega}, \quad (3.2)$$

where C is a positive constant independent of all the foregoing variables.

(b) Assume that there exists a convex domain Ξ such that $\bar{\Omega} \subseteq \Xi$ and $\Gamma_N \subseteq \partial\Xi$. Then, for each $\mathbf{q} \in \mathbf{H}_{\Gamma_N}(\text{div}; \Omega)$ there exist $\boldsymbol{\zeta} \in \mathbf{H}^1(\Omega)$ and $\chi \in \mathbf{H}_{\Gamma_N}^1(\Omega)$ such that

$$\mathbf{q} = \boldsymbol{\zeta} + \mathbf{curl} \chi \quad \text{in } \Omega \quad \text{and} \quad \|\boldsymbol{\zeta}\|_{1,\Omega} + \|\chi\|_{1,\Omega} \leq C \|\mathbf{q}\|_{\text{div}; \Omega}, \quad (3.3)$$

where C is a positive constant independent of all the foregoing variables, and

$$\mathbf{H}_{\Gamma_N}^1(\Omega) := \left\{ \eta \in \mathbf{H}^1(\Omega) : \eta = 0 \quad \text{on } \Gamma_N \right\}.$$

Proof. For the proof of (a) we refer to [25, Lemma 3.7], whereas (b) follows from [1, Lemma 3.9]. We omit further details. \square

3.2 The main result

In what follows we assume that the hypotheses of Theorems 2.1 and 2.2, hold and let $(\mathbf{t}, \mathbf{u}, \mathbf{p}, \theta) \in \mathbb{H} \times \mathbf{H}_0^1(\Omega) \times \mathbf{H}_{\Gamma_N}(\text{div}; \Omega) \times \mathbf{H}^1(\Omega)$ and $(\mathbf{t}_h, \mathbf{u}_h, \mathbf{p}_h, \theta_h) \in \mathbb{H}_h \times \mathbf{H}_h^{\mathbf{u}} \times \mathbf{H}_h^{\mathbf{p}} \times \mathbf{H}_h^{\theta}$ be the unique solutions of problems (2.11) and (2.21), respectively. Then, we define for each $T \in \mathcal{T}_h$ the local a posteriori error indicators

$$\begin{aligned} \tilde{\Theta}_{1,T}^2 &:= \left\| \boldsymbol{\sigma}_h^{\mathbf{d}} - \mu(\theta_h) \mathbf{t}_h \right\|_{0,T}^2 + \|\mathbf{f} + \mathbf{div} \boldsymbol{\sigma}_h\|_{0,T}^2 + \|\boldsymbol{\sigma}_h - \boldsymbol{\sigma}_h^{\mathbf{t}}\|_{0,T}^2 \\ &+ \|\mathbf{t}_h - \mathbf{e}(\mathbf{u}_h)\|_{0,T}^2 + \|\boldsymbol{\rho}_h - (\nabla \mathbf{u}_h - \mathbf{e}(\mathbf{u}_h))\|_{0,T}^2 + \|g + \mathbf{div} \mathbf{p}_h\|_{0,T}^2 \\ &+ \|\nabla \theta_h - (\kappa^{-1} \mathbf{p}_h + \kappa^{-1} \theta_h \mathbf{u}_h)\|_{0,T}^2 + \sum_{e \in \mathcal{E}(T) \cap \mathcal{E}_h(\Gamma_D)} \|\theta_D - \theta_h\|_{0,e}^2, \end{aligned} \quad (3.4)$$

$$\Theta_{1,T}^2 := \tilde{\Theta}_{1,T}^2 + \|\nabla \mathbf{u}_h - (\mathbf{t}_h + \boldsymbol{\rho}_h)\|_{0,T}^2, \quad (3.5)$$

and

$$\begin{aligned} \Theta_{2,T}^2 &:= \tilde{\Theta}_{1,T}^2 + \|\mathbf{f} - \mathbf{P}_h(\mathbf{f})\|_{0,T}^2 + \|g - \mathcal{P}_h(g)\|_{0,T}^2 + h_T^2 \|\nabla \mathbf{u}_h - (\mathbf{t}_h + \boldsymbol{\rho}_h)\|_{0,T}^2 \\ &+ h_T^2 \|\mathbf{rot}(\mathbf{t}_h + \boldsymbol{\rho}_h)\|_{0,T}^2 + h_T^2 \|\mathbf{rot}(\kappa^{-1} \mathbf{p}_h + \kappa^{-1} \theta_h \mathbf{u}_h)\|_{0,T}^2 \\ &+ \sum_{e \in \mathcal{E}(T)} h_e \|\llbracket (\mathbf{t}_h + \boldsymbol{\rho}_h) \mathbf{s} \rrbracket\|_{0,e}^2 + \sum_{e \in \mathcal{E}(T) \cap \mathcal{E}_h(\Omega)} h_e \|\llbracket (\kappa^{-1} \mathbf{p}_h + \kappa^{-1} \theta_h \mathbf{u}_h) \cdot \mathbf{s} \rrbracket\|_{0,e}^2 \\ &+ \sum_{e \in \mathcal{E}(T) \cap \mathcal{E}_h(\Gamma_D)} h_e \left\| \frac{d\theta_D}{ds} - (\kappa^{-1} \mathbf{p}_h + \kappa^{-1} \theta_h \mathbf{u}_h) \cdot \mathbf{s} \right\|_{0,e}^2, \end{aligned} \quad (3.6)$$

so that the global a posteriori error estimators are given, respectively, by

$$\Theta_1 := \left\{ \sum_{T \in \mathcal{T}_h} \Theta_{1,T}^2 + \|\theta_D - \theta_h\|_{1/2, \Gamma_D}^2 \right\}^{1/2} \quad \text{and} \quad \Theta_2 := \left\{ \sum_{T \in \mathcal{T}_h} \Theta_{2,T}^2 \right\}^{1/2}. \quad (3.7)$$

Note that the last term defining $\Theta_{2,T}^2$ (cf. (3.6)) requires that $\frac{d\theta_D}{ds} \Big|_e \in L^2(e)$ for each $e \in \mathcal{E}_h(\Gamma_D)$. This is ensured below by assuming that $\theta_D \in \mathbf{H}^1(\Gamma_D)$.

The main goal of the present Section 3 is to establish, under suitable assumptions, the existence of positive constants $C_{\text{rel}}, C_{\text{eff}}, \tilde{C}_{\text{rel}}$, and \tilde{C}_{eff} , independent of the meshsizes and the continuous and discrete solutions, such that

$$C_{\text{eff}} \Theta_1 \leq \|(\mathbf{t}, \mathbf{u}, \mathbf{p}, \theta) - (\mathbf{t}_h, \mathbf{u}_h, \mathbf{p}_h, \theta_h)\| \leq C_{\text{rel}} \Theta_1, \quad (3.8)$$

and

$$\tilde{C}_{\text{eff}}\Theta_2 \leq \|(\underline{\mathbf{t}}, \mathbf{u}, \mathbf{p}, \theta) - (\underline{\mathbf{t}}_h, \mathbf{u}_h, \mathbf{p}_h, \theta_h)\| \leq \tilde{C}_{\text{rel}}\Theta_2. \quad (3.9)$$

The upper and lower bounds in (3.8) and (3.9), which are known as the reliability and efficiency of the estimators Θ_1 and Θ_2 , are derived below in Section 3.4 and 3.5, respectively, under the assumption that θ_D is piecewise polynomials on the induced triangulation on Γ_D . Otherwise, higher order terms arising from polynomial approximations of these functions would appear in (3.8) and (3.9).

At this point we remark that for the derivation of the first a posteriori error estimator we will use the fact that $\mathbf{u} \in \mathbf{H}_0^1(\Omega)$ and $\theta \in \mathbf{H}^1(\Omega)$, so that we can integrate some terms by parts in the whole domain Ω . In turn, for the second estimator we exploit the properties of the Helmholtz decompositions (cf. Lemma 3.3) jointly with the Clément and Raviart–Thomas operators, whence new terms capturing the jumps across the sides/edges of the triangulation appear.

3.3 A general a posteriori error estimate

In order to establish the reliability estimates of the a posteriori error estimators Θ_1 and Θ_2 , that is the upper bounds in (3.8) and (3.9), we first bound the unknowns related to the fluid and the heat by applying the uniform ellipticity of the bilinear forms of the continuous formulation, and then we conclude a preliminary upper bound for the total error by assuming that the data are small enough. More precisely, we begin with the following auxiliary result.

Lemma 3.4 *There exists $C > 0$, independent of h , such that*

$$\begin{aligned} \|(\underline{\mathbf{t}}, \mathbf{u}) - (\underline{\mathbf{t}}_h, \mathbf{u}_h)\| &\leq C \left\{ \left\| \boldsymbol{\sigma}_h^{\text{d}} - \mu(\theta_h)\mathbf{t}_h \right\|_{0,\Omega} + \|\mathbf{f} + \mathbf{div} \boldsymbol{\sigma}_h\|_{0,\Omega} + \|\boldsymbol{\sigma}_h - \boldsymbol{\sigma}_h^{\text{t}}\|_{0,\Omega} \right. \\ &+ \|\mathbf{t}_h - \mathbf{e}(\mathbf{u}_h)\|_{0,\Omega} + \|\boldsymbol{\rho}_h - (\nabla \mathbf{u}_h - \mathbf{e}(\mathbf{u}_h))\|_{0,\Omega} + \|\mathcal{R}_f\|_{\mathbb{H}_0(\mathbf{div};\Omega)'} \left. \right\} \\ &+ \frac{2}{\alpha(\Omega)} L_\mu (1 + \kappa_1^2)^{1/2} \tilde{C}_{\mathbf{S}} C_\delta \tilde{C}_\delta \|\mathbf{f}\|_{\delta,\Omega} \|\theta - \theta_h\|_{1,\Omega}, \end{aligned} \quad (3.10)$$

where $\mathcal{R}_f : \mathbb{H}_0(\mathbf{div};\Omega) \rightarrow \mathbb{R}$ is the functional defined by

$$\begin{aligned} \mathcal{R}_f(\boldsymbol{\tau}) &:= -\kappa_1 \int_\Omega \left\{ \boldsymbol{\sigma}_h^{\text{d}} - \mu(\theta_h)\mathbf{t}_h \right\} : \boldsymbol{\tau}^{\text{d}} - \kappa_2 \int_\Omega \left\{ \mathbf{f} + \mathbf{div} \boldsymbol{\sigma}_h \right\} \cdot \mathbf{div} \boldsymbol{\tau} \\ &\quad - \int_\Omega (\mathbf{t}_h + \boldsymbol{\rho}_h) : \boldsymbol{\tau}^{\text{d}} - \int_\Omega \mathbf{u}_h \cdot \mathbf{div} \boldsymbol{\tau}, \end{aligned} \quad (3.11)$$

which satisfies

$$\mathcal{R}_f(\boldsymbol{\tau}_h) = 0 \quad \forall \boldsymbol{\tau}_h \in \mathbb{H}_h^\sigma. \quad (3.12)$$

Proof. According to [6, Lemma 3.1], we have that the bilinear form \mathbf{A}_θ is uniformly elliptic on $\mathbb{H} \times \mathbf{H}_0^1(\Omega)$ with a positive constant $\alpha(\Omega)$. This implies that

$$\alpha(\Omega) \|(\underline{\mathbf{t}}, \mathbf{u}) - (\underline{\mathbf{t}}_h, \mathbf{u}_h)\| \leq \sup_{\substack{(\underline{\mathbf{r}}, \mathbf{v}) \in \mathbb{H} \times \mathbf{H}_0^1(\Omega) \\ (\underline{\mathbf{r}}, \mathbf{v}) \neq \mathbf{0}}} \frac{\mathbf{A}_\theta((\underline{\mathbf{t}}, \mathbf{u}) - (\underline{\mathbf{t}}_h, \mathbf{u}_h), (\underline{\mathbf{r}}, \mathbf{v}))}{\|(\underline{\mathbf{r}}, \mathbf{v})\|}. \quad (3.13)$$

In turn, in order to estimate the right-hand side in (3.13), we first add and subtract suitable terms to write

$$\begin{aligned} &\mathbf{A}_\theta((\underline{\mathbf{t}}, \mathbf{u}) - (\underline{\mathbf{t}}_h, \mathbf{u}_h), (\underline{\mathbf{r}}, \mathbf{v})) \\ &= \mathbf{F}(\underline{\mathbf{r}}, \mathbf{v}) - \mathbf{A}_{\theta_h}((\underline{\mathbf{t}}_h, \mathbf{u}_h), (\underline{\mathbf{r}}, \mathbf{v})) - (\mathbf{A}_\theta - \mathbf{A}_{\theta_h})((\underline{\mathbf{t}}_h, \mathbf{u}_h), (\underline{\mathbf{r}}, \mathbf{v})), \end{aligned}$$

and then proceed similarly to [1, eq. (3.15)]. Indeed, from the definitions of \mathbf{A}_θ and \mathbf{F} (cf. (2.12) and (2.15), respectively), and employing the Cauchy–Schwarz inequality, the estimate given by [6, eq. (3.24)] for $|(\mathbf{A}_\theta - \mathbf{A}_{\theta_h})(\cdot, (\underline{\mathbf{r}}, \mathbf{v}))|$, and the regularity assumption [6, eq. (3.22)], we deduce that

$$\begin{aligned} \frac{|\mathbf{A}_\theta((\underline{\mathbf{t}}, \mathbf{u}) - (\underline{\mathbf{t}}_h, \mathbf{u}_h), (\underline{\mathbf{r}}, \mathbf{v}))|}{\|(\underline{\mathbf{r}}, \mathbf{v})\|} &\leq C \left\{ \left\| \boldsymbol{\sigma}_h^{\mathbf{d}} - \mu(\theta_h) \mathbf{t}_h \right\|_{0,\Omega} + \|\mathbf{f} + \mathbf{div} \boldsymbol{\sigma}_h\|_{0,\Omega} \right. \\ &+ \left\| \boldsymbol{\sigma}_h - \boldsymbol{\sigma}_h^{\mathbf{t}} \right\|_{0,\Omega} + \|\mathbf{t}_h - \mathbf{e}(\mathbf{u}_h)\|_{0,\Omega} + \|\boldsymbol{\rho}_h - (\nabla \mathbf{u}_h - \mathbf{e}(\mathbf{u}_h))\|_{0,\Omega} + \|\mathcal{R}_f\|_{\mathbb{H}_0(\mathbf{div}; \Omega)'} \left. \right\} \\ &+ 2L_\mu(1 + \kappa_1^2)^{1/2} \widehat{C}_{\mathbf{S}} C_\delta \widetilde{C}_\delta \|\mathbf{f}\|_{\delta, \Omega} \|\theta - \theta_h\|_{1,\Omega}, \end{aligned} \quad (3.14)$$

where $\widehat{C}_{\mathbf{S}}$, C_δ , and \widetilde{C}_δ are the constants provided by [6, eqs. (3.22), (3.25), and (3.32)], respectively. In this way, replacing the inequality (3.14) into (3.13), we get (3.10). Moreover, using the fact that

$$\mathbf{F}(\underline{\mathbf{r}}_h, \mathbf{v}_h) - \mathbf{A}_{\theta_h}((\underline{\mathbf{t}}_h, \mathbf{u}_h), (\underline{\mathbf{r}}_h, \mathbf{v}_h)) = 0 \quad \forall (\underline{\mathbf{r}}_h, \mathbf{v}_h) \in \mathbb{H}_h \times \mathbf{H}_h^{\mathbf{u}},$$

and taking in particular $\underline{\mathbf{r}}_h = (\mathbf{0}, \boldsymbol{\tau}_h, \mathbf{0})$ and $\mathbf{v}_h = \mathbf{0}$, we get (3.12), which completes the proof. \square

Next, we derive an analogous preliminary bound for the error associated to the heat variables.

Lemma 3.5 *There exists $C > 0$, independent of h , such that*

$$\begin{aligned} \|(\mathbf{p}, \theta) - (\mathbf{p}_h, \theta_h)\| &\leq C \left\{ \|g + \mathbf{div} \mathbf{p}_h\|_{0,\Omega} + \|\nabla \theta_h - (\kappa^{-1} \mathbf{p}_h + \kappa^{-1} \theta_h \mathbf{u}_h)\|_{0,\Omega} \right. \\ &+ \|\theta_D - \theta_h\|_{0,\Gamma_D} + \|\mathcal{R}_h\|_{\mathbf{H}_{\Gamma_N}(\mathbf{div}; \Omega)'} \left. \right\} + \frac{2}{\widetilde{\alpha}(\Omega)} \kappa^{-1} (1 + \kappa_5^2)^{1/2} c(\Omega) \|\theta_h\|_{1,\Omega} \|\mathbf{u} - \mathbf{u}_h\|_{1,\Omega}, \end{aligned} \quad (3.15)$$

where $\mathcal{R}_h : \mathbf{H}_{\Gamma_N}(\mathbf{div}; \Omega) \rightarrow \mathbb{R}$ is the functional defined by

$$\mathcal{R}_h(\mathbf{q}) := -\kappa_6 \int_{\Omega} \left\{ g + \mathbf{div} \mathbf{p}_h \right\} \mathbf{div} \mathbf{q} - \int_{\Omega} \left\{ \kappa^{-1} \mathbf{p}_h + \kappa^{-1} \theta_h \mathbf{u}_h \right\} \cdot \mathbf{q} - \int_{\Omega} \theta_h \mathbf{div} \mathbf{q} + \langle \mathbf{q} \cdot \mathbf{n}, \theta_D \rangle_{\Gamma_D}, \quad (3.16)$$

which satisfies

$$\mathcal{R}_h(\mathbf{q}_h) = 0 \quad \forall \mathbf{q}_h \in \mathbf{H}_h^{\mathbf{p}}. \quad (3.17)$$

Proof. According to [6, Lemma 3.2] and using the fact that $\|\mathbf{u}\|_{1,\Omega} \leq c_{\mathbf{S}} \|\mathbf{f}\|_{0,\Omega}$ (cf. (2.18)), we have that the bilinear form $\widetilde{\mathbf{A}} + \widetilde{\mathbf{B}}_{\mathbf{u}}$ is uniformly elliptic on $\mathbf{H}_{\Gamma_N}(\mathbf{div}; \Omega) \times \mathbf{H}^1(\Omega)$ with a positive constant $\widetilde{\alpha}(\Omega)/2$. This implies that

$$\frac{\widetilde{\alpha}(\Omega)}{2} \|(\mathbf{p}, \theta) - (\mathbf{p}_h, \theta_h)\| \leq \sup_{\substack{(\mathbf{q}, \psi) \in \mathbf{H}_{\Gamma_N}(\mathbf{div}; \Omega) \times \mathbf{H}^1(\Omega) \\ (\mathbf{q}, \psi) \neq \mathbf{0}}} \frac{(\widetilde{\mathbf{A}} + \widetilde{\mathbf{B}}_{\mathbf{u}})((\mathbf{p}, \theta) - (\mathbf{p}_h, \theta_h), (\mathbf{q}, \psi))}{\|(\mathbf{q}, \psi)\|}. \quad (3.18)$$

In turn, in order to estimate the right-hand side in (3.18), we add and subtract suitable terms to write

$$\begin{aligned} &(\widetilde{\mathbf{A}} + \widetilde{\mathbf{B}}_{\mathbf{u}})((\mathbf{p}, \theta) - (\mathbf{p}_h, \theta_h), (\mathbf{q}, \psi)) \\ &= \widetilde{\mathbf{F}}(\mathbf{q}, \psi) - (\widetilde{\mathbf{A}} + \widetilde{\mathbf{B}}_{\mathbf{u}_h})((\mathbf{p}_h, \theta_h), (\mathbf{q}, \psi)) - \widetilde{\mathbf{B}}_{\mathbf{u}-\mathbf{u}_h}((\mathbf{p}_h, \theta_h), (\mathbf{q}, \psi)), \end{aligned}$$

whence, using the definitions of $\widetilde{\mathbf{A}}$, $\widetilde{\mathbf{B}}_{\mathbf{w}}$, and $\widetilde{\mathbf{F}}$ (cf. (2.13), (2.14), and (2.16), respectively), the continuity of $\widetilde{\mathbf{B}}_{\mathbf{u}-\mathbf{u}_h}$ (see [6, eq. (3.16)]), and the Cauchy–Schwarz inequality, we find that

$$\begin{aligned} \frac{|(\widetilde{\mathbf{A}} + \widetilde{\mathbf{B}}_{\mathbf{u}})((\mathbf{p}, \theta) - (\mathbf{p}_h, \theta_h), (\mathbf{q}, \psi))|}{\|(\mathbf{q}, \psi)\|} &\leq C \left\{ \|g + \mathbf{div} \mathbf{p}_h\|_{0,\Omega} + \|\nabla \theta_h - (\kappa^{-1} \mathbf{p}_h + \kappa^{-1} \theta_h \mathbf{u}_h)\|_{0,\Omega} \right. \\ &+ \|\theta_D - \theta_h\|_{0,\Gamma_D} + \|\mathcal{R}_h\|_{\mathbf{H}_{\Gamma_N}(\mathbf{div}; \Omega)'} \left. \right\} + \kappa^{-1} (1 + \kappa_5^2)^{1/2} c(\Omega) \|\theta_h\|_{1,\Omega} \|\mathbf{u} - \mathbf{u}_h\|_{1,\Omega}, \end{aligned} \quad (3.19)$$

where $c(\Omega)$ is the constant in [6, eq. (2.15)]. Then, replacing the inequality (3.19) into (3.18), we obtain (3.15). Finally, using the fact that

$$\tilde{\mathbf{F}}(\mathbf{q}_h, \psi_h) - (\tilde{\mathbf{A}} + \tilde{\mathbf{B}}_{\mathbf{u}_h})(\mathbf{p}_h, \theta_h), (\mathbf{q}_h, \psi_h) = 0 \quad \forall (\mathbf{q}_h, \psi_h) \in \mathbf{H}_h^{\mathbf{p}} \times \mathbf{H}_h^{\theta},$$

and taking in particular $\psi_h = 0$, we arrive at (3.17), which completes the proof. \square

We now combine the inequalities provided by Lemmas 3.4 and 3.5 to derive a preliminary upper bound for the total error $\|(\underline{\mathbf{t}}, \mathbf{u}, \mathbf{p}, \theta) - (\underline{\mathbf{t}}_h, \mathbf{u}_h, \mathbf{p}_h, \theta_h)\|$. Indeed, by gathering together the estimates (3.10) and (3.15), and noting the fact that $\theta_h \in \mathcal{W}_h$, it follows that

$$\begin{aligned} & \|(\underline{\mathbf{t}}, \mathbf{u}, \mathbf{p}, \theta) - (\underline{\mathbf{t}}_h, \mathbf{u}_h, \mathbf{p}_h, \theta_h)\| \leq \mathbf{C}(\mathbf{f}, g, \theta_D) \|(\underline{\mathbf{t}}, \mathbf{u}, \mathbf{p}, \theta) - (\underline{\mathbf{t}}_h, \mathbf{u}_h, \mathbf{p}_h, \theta_h)\| \\ & + C \left\{ \left\| \boldsymbol{\sigma}_h^{\text{d}} - \mu(\theta_h) \mathbf{t}_h \right\|_{0,\Omega} + \|\mathbf{f} + \mathbf{div} \boldsymbol{\sigma}_h\|_{0,\Omega} + \|\boldsymbol{\sigma}_h - \boldsymbol{\sigma}_h^{\text{t}}\|_{0,\Omega} + \|\mathbf{t}_h - \mathbf{e}(\mathbf{u}_h)\|_{0,\Omega} \right. \\ & + \|\boldsymbol{\rho}_h - (\nabla \mathbf{u}_h - \mathbf{e}(\mathbf{u}_h))\|_{0,\Omega} + \|g + \mathbf{div} \mathbf{p}_h\|_{0,\Omega} + \|\nabla \theta_h - (\kappa^{-1} \mathbf{p}_h + \kappa^{-1} \theta_h \mathbf{u}_h)\|_{0,\Omega} \\ & \left. + \|\theta_D - \theta_h\|_{0,\Gamma_D} + \|\mathcal{R}_f\|_{\mathbb{H}_0(\mathbf{div};\Omega)'} + \|\mathcal{R}_h\|_{\mathbf{H}_{\Gamma_N}(\mathbf{div};\Omega)'} \right\}, \end{aligned} \quad (3.20)$$

where

$$\mathbf{C}(\mathbf{f}, g, \theta_D) := \max \left\{ \mathbf{C}_1(\mathbf{f}, g, \theta_D), \mathbf{C}_2(\mathbf{f}, g, \theta_D) \right\},$$

with

$$\mathbf{C}_1(\mathbf{f}, g, \theta_D) := \frac{2}{\tilde{\alpha}(\Omega)} \kappa^{-1} (1 + \kappa_5^2)^{1/2} c(\Omega) c_{\mathbb{S}} \left\{ \|g\|_{0,\Omega} + \|\theta_D\|_{0,\Gamma_D} + \|\theta_D\|_{1/2,\Gamma_D} \right\}$$

and

$$\mathbf{C}_2(\mathbf{f}, g, \theta_D) := \frac{2}{\alpha(\Omega)} L_{\mu} (1 + \kappa_1^2)^{1/2} \widehat{C}_{\mathbf{S}} C_{\delta} \widetilde{C}_{\delta} \|\mathbf{f}\|_{\delta,\Omega}.$$

Consequently, we can establish the following preliminary upper bound for the total error.

Lemma 3.6 *Assume that the data \mathbf{f}, g and θ_D satisfy:*

$$\mathbf{C}_i(\mathbf{f}, g, \theta_D) \leq \frac{1}{2} \quad \forall i \in \{1, 2\}. \quad (3.21)$$

Then, there exists $C > 0$, depending only on parameters, data and other constants, all of them independent of h , such that

$$\begin{aligned} & \|(\underline{\mathbf{t}}, \mathbf{u}, \mathbf{p}, \theta) - (\underline{\mathbf{t}}_h, \mathbf{u}_h, \mathbf{p}_h, \theta_h)\| \leq C \left\{ \left\| \boldsymbol{\sigma}_h^{\text{d}} - \mu(\theta_h) \mathbf{t}_h \right\|_{0,\Omega} + \|\mathbf{f} + \mathbf{div} \boldsymbol{\sigma}_h\|_{0,\Omega} \right. \\ & + \|\boldsymbol{\sigma}_h - \boldsymbol{\sigma}_h^{\text{t}}\|_{0,\Omega} + \|\mathbf{t}_h - \mathbf{e}(\mathbf{u}_h)\|_{0,\Omega} + \|\boldsymbol{\rho}_h - (\nabla \mathbf{u}_h - \mathbf{e}(\mathbf{u}_h))\|_{0,\Omega} + \|g + \mathbf{div} \mathbf{p}_h\|_{0,\Omega} \\ & \left. + \|\nabla \theta_h - (\kappa^{-1} \mathbf{p}_h + \kappa^{-1} \theta_h \mathbf{u}_h)\|_{0,\Omega} + \|\theta_D - \theta_h\|_{0,\Gamma_D} + \|\mathcal{R}_f\|_{\mathbb{H}_0(\mathbf{div};\Omega)'} + \|\mathcal{R}_h\|_{\mathbf{H}_{\Gamma_N}(\mathbf{div};\Omega)'} \right\}. \end{aligned} \quad (3.22)$$

Proof. It follows from a direct application of the assumption (3.21) in the inequality (3.20). \square

We end this section with equivalent definitions of the functionals \mathcal{R}_f and \mathcal{R}_h . In fact, noting that $\mathbf{t}_h : \mathbb{I} = \text{tr} \mathbf{t}_h = 0$ and $\boldsymbol{\rho}_h : \mathbb{I} = 0$, we first observe that

$$\int_{\Omega} (\mathbf{t}_h + \boldsymbol{\rho}_h) : \boldsymbol{\tau}^{\text{d}} = \int_{\Omega} (\mathbf{t}_h + \boldsymbol{\rho}_h)^{\text{d}} : \boldsymbol{\tau} = \int_{\Omega} (\mathbf{t}_h + \boldsymbol{\rho}_h) : \boldsymbol{\tau}.$$

In this way, given $\boldsymbol{\tau} \in \mathbb{H}_0(\mathbf{div}; \Omega)$, we integrate by parts the expression $\int_{\Omega} \mathbf{u}_h \cdot \mathbf{div} \boldsymbol{\tau}$ and use the homogeneous Dirichlet boundary condition on Γ of $\mathbf{u}_h \in \mathbf{H}_h^{\mathbf{u}}$ (cf. (2.20)), to find that

$$\mathcal{R}_f(\boldsymbol{\tau}) = -\kappa_1 \int_{\Omega} \left\{ \boldsymbol{\sigma}_h^d - \mu(\theta_h) \mathbf{t}_h \right\} : \boldsymbol{\tau} - \kappa_2 \int_{\Omega} \left\{ \mathbf{f} + \mathbf{div} \boldsymbol{\sigma}_h \right\} \cdot \mathbf{div} \boldsymbol{\tau} + \int_{\Omega} \left\{ \nabla \mathbf{u}_h - (\mathbf{t}_h + \boldsymbol{\rho}_h) \right\} : \boldsymbol{\tau}. \quad (3.23)$$

Analogously, given $\mathbf{q} \in \mathbf{H}_{\Gamma_N}(\mathbf{div}; \Omega)$, we integrate by parts the expression $\int_{\Omega} \theta_h \mathbf{div} \mathbf{q}$ and use now the homogeneous Neumann boundary condition of \mathbf{q} on Γ_N , to arrive at

$$\mathcal{R}_h(\mathbf{q}) = -\kappa_6 \int_{\Omega} \left\{ g + \mathbf{div} \mathbf{p}_h \right\} \mathbf{div} \mathbf{q} + \int_{\Omega} \left\{ \nabla \theta_h - (\kappa^{-1} \mathbf{p}_h + \kappa^{-1} \theta_h \mathbf{u}_h) \right\} \cdot \mathbf{q} + \langle \mathbf{q} \cdot \mathbf{n}, \theta_D - \theta_h \rangle_{\Gamma_D}. \quad (3.24)$$

3.4 Reliability of the a posteriori error estimators

We now proceed to bound the norms of the functionals \mathcal{R}_f and \mathcal{R}_h appearing on the right-hand side of (3.22), by conveniently considering either their original definitions or the new expressions (3.23) and (3.24), respectively. This task is actually performed in two different ways, which leads to the reliability of the a posteriori error estimators Θ_1 and Θ_2 . We begin with Θ_1 .

Theorem 3.7 *Assume that the data \mathbf{f}, g and θ_D satisfy (3.21). Then there exist $C_{\text{rel}} > 0$, independent of h , such that*

$$\|(\mathbf{t}, \mathbf{u}, \mathbf{p}, \theta) - (\mathbf{t}_h, \mathbf{u}_h, \mathbf{p}_h, \theta_h)\| \leq C_{\text{rel}} \Theta_1. \quad (3.25)$$

Proof. We first observe that, employing Cauchy–Schwarz inequality and recalling that $\langle \cdot, \cdot \rangle_{\Gamma_D}$ stands for the duality pairing between $\mathbf{H}^{-1/2}(\Gamma_D)$ and $\mathbf{H}^{1/2}(\Gamma_D)$, we deduce from (3.23) and (3.24) that

$$\|\mathcal{R}_f\|_{\mathbb{H}_0(\mathbf{div}; \Omega)'} \leq c_1 \left\{ \left\| \boldsymbol{\sigma}_h^d - \mu(\theta_h) \mathbf{t}_h \right\|_{0, \Omega} + \|\mathbf{f} + \mathbf{div} \boldsymbol{\sigma}_h\|_{0, \Omega} + \|\nabla \mathbf{u}_h - (\mathbf{t}_h + \boldsymbol{\rho}_h)\|_{0, \Omega} \right\} \quad (3.26)$$

and

$$\|\mathcal{R}_h\|_{\mathbf{H}_{\Gamma_N}(\mathbf{div}; \Omega)'} \leq c_2 \left\{ \|g + \mathbf{div} \mathbf{p}_h\|_{0, \Omega} + \|\nabla \theta_h - (\kappa^{-1} \mathbf{p}_h + \kappa^{-1} \theta_h \mathbf{u}_h)\|_{0, \Omega} + \|\theta_D - \theta_h\|_{1/2, \Gamma_D} \right\}, \quad (3.27)$$

respectively. In this way, the proof follows straightforwardly from the definition of Θ_1 (cf. (3.5)), Lemma 3.6, and inequalities (3.26) and (3.27). \square

Having proved Theorem 3.7, we now aim to establish the reliability of Θ_2 (cf. (3.6)), which is accomplished by applying the Helmholtz decompositions provided by Lemma 3.3 to bound $\|\mathcal{R}_f\|_{\mathbb{H}_0(\mathbf{div}; \Omega)'} and $\|\mathcal{R}_h\|_{\mathbf{H}_{\Gamma_N}(\mathbf{div}; \Omega)'}$. Actually, in what follows we provide the details only for \mathcal{R}_f since those for \mathcal{R}_h follow analogously. In fact, given $\boldsymbol{\tau} \in \mathbb{H}_0(\mathbf{div}; \Omega)$, and thanks to part (a) of Lemma 3.3, we first let $\mathbf{z} \in \mathbf{H}^2(\Omega)$ and $\boldsymbol{\varphi} \in \mathbf{H}^1(\Omega)$ be such that $\boldsymbol{\tau} = \nabla \mathbf{z} + \mathbf{curl} \boldsymbol{\varphi}$ in Ω , and$

$$\|\mathbf{z}\|_{2, \Omega} + \|\boldsymbol{\varphi}\|_{1, \Omega} \leq C \|\boldsymbol{\tau}\|_{\mathbf{div}; \Omega}, \quad (3.28)$$

and then define $\boldsymbol{\tau}_h := \boldsymbol{\Pi}_h(\nabla \mathbf{z}) + \mathbf{curl}(\mathbf{I}_h \boldsymbol{\varphi}) + c\mathbb{I}$, where $c \in \mathbb{R}$ is chosen so that $\boldsymbol{\tau}_h$ belongs to $\mathbb{H}_h^{\boldsymbol{\sigma}}$ (cf. Section 3.1). Hence, employing from (3.12) that $\mathcal{R}_f(\boldsymbol{\tau}_h) = 0$, it readily follows from the foregoing expressions that $\mathcal{R}_f(\boldsymbol{\tau})$ can be decomposed as

$$\mathcal{R}_f(\boldsymbol{\tau}) = \mathcal{R}_f(\boldsymbol{\tau} - \boldsymbol{\tau}_h) = \mathcal{R}_f(\nabla \mathbf{z} - \boldsymbol{\Pi}_h(\nabla \mathbf{z})) + \mathcal{R}_f(\mathbf{curl}(\boldsymbol{\varphi} - \mathbf{I}_h \boldsymbol{\varphi})). \quad (3.29)$$

Consequently, we now require to bound the terms on the right-hand side of (3.29), which is done in the following two lemmas.

Lemma 3.8 *There exists $C > 0$, independent of h , such that for each $\mathbf{z} \in \mathbf{H}^2(\Omega)$ there holds*

$$\left| \mathcal{R}_f(\nabla \mathbf{z} - \mathbf{\Pi}_h(\nabla \mathbf{z})) \right| \leq C \left\{ \sum_{T \in \mathcal{T}_h} \tilde{\Theta}_{f,T}^2 \right\}^{1/2} \|\mathbf{z}\|_{2,\Omega},$$

where

$$\tilde{\Theta}_{f,T}^2 = h_T^2 \left\| \boldsymbol{\sigma}_h^d - \mu(\theta_h) \mathbf{t}_h \right\|_{0,T}^2 + \|\mathbf{f} - \mathbf{P}_h(\mathbf{f})\|_{0,T}^2 + h_T^2 \|\nabla \mathbf{u}_h - (\mathbf{t}_h + \boldsymbol{\rho}_h)\|_{0,T}^2. \quad (3.30)$$

Proof. Using the alternative definition of the functional \mathcal{R}_f (cf. (3.23)), the proof follows from a slight modification of that of [25, Lemma 3.10]. We omit further details. \square

Lemma 3.9 *There exists $C > 0$, independent of h , such that for each $\boldsymbol{\varphi} \in \mathbf{H}^1(\Omega)$ there holds*

$$\left| \mathcal{R}_f(\mathbf{curl}(\boldsymbol{\varphi} - \mathbf{I}_h \boldsymbol{\varphi})) \right| \leq C \left\{ \sum_{T \in \mathcal{T}_h} \hat{\Theta}_{f,T}^2 \right\}^{1/2} \|\boldsymbol{\varphi}\|_{1,\Omega},$$

where

$$\hat{\Theta}_{f,T}^2 = \left\| \boldsymbol{\sigma}_h^d - \mu(\theta_h) \mathbf{t}_h \right\|_{0,T}^2 + h_T^2 \|\mathbf{rot}(\mathbf{t}_h + \boldsymbol{\rho}_h)\|_{0,T}^2 + \sum_{e \in \mathcal{E}(T)} h_e \|\llbracket (\mathbf{t}_h + \boldsymbol{\rho}_h) \mathbf{s} \rrbracket\|_{0,e}^2. \quad (3.31)$$

Proof. Given $\boldsymbol{\varphi} \in \mathbf{H}^1(\Omega)$, we first notice from the original definition (3.11) of \mathcal{R}_f that there holds

$$\mathcal{R}_f(\mathbf{curl}(\boldsymbol{\varphi} - \mathbf{I}_h \boldsymbol{\varphi})) = -\kappa_1 \int_{\Omega} \left\{ \boldsymbol{\sigma}_h^d - \mu(\theta_h) \mathbf{t}_h \right\} : \mathbf{curl}(\boldsymbol{\varphi} - \mathbf{I}_h \boldsymbol{\varphi}) - \int_{\Omega} (\mathbf{t}_h + \boldsymbol{\rho}_h) : \mathbf{curl}(\boldsymbol{\varphi} - \mathbf{I}_h \boldsymbol{\varphi}). \quad (3.32)$$

Then, for estimating the first term on the right-hand side of (3.32) we proceed as in the proof of [25, Lemma 3.9] and apply the boundedness of $\mathbf{I}_h : \mathbf{H}^1(\Omega) \rightarrow \mathbf{H}^1(\Omega)$ ([16, Lemma 1.127, pag. 69]), as well as the Cauchy–Schwarz and triangle inequalities, to obtain

$$\left| \kappa_1 \int_{\Omega} \left\{ \boldsymbol{\sigma}_h^d - \mu(\theta_h) \mathbf{t}_h \right\} : \mathbf{curl}(\boldsymbol{\varphi} - \mathbf{I}_h \boldsymbol{\varphi}) \right| \leq C \left\{ \sum_{T \in \mathcal{T}_h} \left\| \boldsymbol{\sigma}_h^d - \mu(\theta_h) \mathbf{t}_h \right\|_{0,T}^2 \right\}^{1/2} \|\boldsymbol{\varphi}\|_{1,\Omega}. \quad (3.33)$$

Next, analogously to the proof of [25, Lemma 3.9], we decompose the second term on the right-hand side of (3.32) according to the triangulation \mathcal{T}_h , and integrate by parts on each $T \in \mathcal{T}_h$ to obtain

$$\int_{\Omega} (\mathbf{t}_h + \boldsymbol{\rho}_h) : \mathbf{curl}(\boldsymbol{\varphi} - \mathbf{I}_h \boldsymbol{\varphi}) = \sum_{T \in \mathcal{T}_h} \int_T \mathbf{rot}(\mathbf{t}_h + \boldsymbol{\rho}_h) \cdot (\boldsymbol{\varphi} - \mathbf{I}_h \boldsymbol{\varphi}) - \sum_{e \in \mathcal{E}_h} \int_e \llbracket (\mathbf{t}_h + \boldsymbol{\rho}_h) \mathbf{s} \rrbracket \cdot (\boldsymbol{\varphi} - \mathbf{I}_h \boldsymbol{\varphi}).$$

In this way, applying the Cauchy–Schwarz inequality, the approximation properties of the Clément interpolator \mathbf{I}_h (cf. Lemma 3.2), and the fact that the number of triangles of the macro-elements $\Delta(T)$ and $\Delta(e)$ are uniformly bounded, we deduce that

$$\begin{aligned} & \left| \int_{\Omega} (\mathbf{t}_h + \boldsymbol{\rho}_h) : \mathbf{curl}(\boldsymbol{\varphi} - \mathbf{I}_h \boldsymbol{\varphi}) \right| \\ & \leq C \sum_{T \in \mathcal{T}_h} \left\{ h_T^2 \|\mathbf{rot}(\mathbf{t}_h + \boldsymbol{\rho}_h)\|_{0,T}^2 + \sum_{e \in \mathcal{E}(T)} h_e \|\llbracket (\mathbf{t}_h + \boldsymbol{\rho}_h) \mathbf{s} \rrbracket\|_{0,e}^2 \right\}^{1/2} \|\boldsymbol{\varphi}\|_{1,\Omega}. \end{aligned} \quad (3.34)$$

Finally, by replacing the inequalities (3.33) and (3.34) into (3.32) we conclude the proof. \square

As a direct consequence of Lemmas 3.8 and 3.9, and the stability estimate (3.28) for the Helmholtz decomposition, we obtain the following upper bound for $\|\mathcal{R}_f\|_{\mathbb{H}_0(\mathbf{div};\Omega)}$.

Lemma 3.10 *There exists $C > 0$, independent of h , such that*

$$\|\mathcal{R}_f\|_{\mathbb{H}_0(\text{div};\Omega)'} \leq C \left\{ \sum_{T \in \mathcal{T}_h} \Theta_{f,T}^2 \right\}^{1/2},$$

where

$$\begin{aligned} \Theta_{f,T}^2 := & \left\| \boldsymbol{\sigma}_h^d - \mu(\theta_h) \mathbf{t}_h \right\|_{0,T}^2 + \|\mathbf{f} - \mathbf{P}_h(\mathbf{f})\|_{0,T}^2 + h_T^2 \|\nabla \mathbf{u}_h - (\mathbf{t}_h + \boldsymbol{\rho}_h)\|_{0,T}^2 \\ & + h_T^2 \|\mathbf{rot}(\mathbf{t}_h + \boldsymbol{\rho}_h)\|_{0,T}^2 + \sum_{e \in \mathcal{E}(T)} h_e \|\llbracket (\mathbf{t}_h + \boldsymbol{\rho}_h) \mathbf{s} \rrbracket\|_{0,e}^2. \end{aligned} \quad (3.35)$$

Proof. It suffices to see that the first term defining $\tilde{\Theta}_{f,T}^2$ (cf. (3.30) in Lemma 3.8) is dominated by the first term of $\hat{\Theta}_{f,T}^2$ (cf. (3.31) in Lemma 3.9), which explains the subtraction of the former in the original definition of $\Theta_{f,T}^2$. \square

Finally, the corresponding estimate for \mathcal{R}_h is given by the following lemma.

Lemma 3.11 *Assume that there exists a convex domain Ξ such that $\bar{\Omega} \subseteq \Xi$ and $\Gamma_N \subseteq \partial\Xi$. Assume further that $\theta_D \in \mathbf{H}^1(\Gamma_D)$. Then there exists $C > 0$, independent of h , such that*

$$\|\mathcal{R}_h\|_{\mathbf{H}_{\Gamma_N}(\text{div};\Omega)'} \leq C \left\{ \sum_{T \in \mathcal{T}_h} \Theta_{h,T}^2 \right\},$$

where

$$\begin{aligned} \Theta_{h,T}^2 := & \|g - \mathcal{P}_h(g)\|_{0,T}^2 + h_T^2 \|\nabla \theta_h - (\kappa^{-1} \mathbf{p}_h + \kappa^{-1} \theta_h \mathbf{u}_h)\|_{0,T}^2 \\ & + h_T^2 \|\mathbf{rot}(\kappa^{-1} \mathbf{p}_h + \kappa^{-1} \theta_h \mathbf{u}_h)\|_{0,T}^2 + \sum_{e \in \mathcal{E}(T) \cap \mathcal{E}_h(\Omega)} h_e \|\llbracket (\kappa^{-1} \mathbf{p}_h + \kappa^{-1} \theta_h \mathbf{u}_h) \cdot \mathbf{s} \rrbracket\|_{0,e}^2 \\ & + \sum_{e \in \mathcal{E}(T) \cap \mathcal{E}_h(\Gamma_D)} h_e \left\{ \left\| \frac{d\theta_D}{ds} - (\kappa^{-1} \mathbf{p}_h + \kappa^{-1} \theta_h \mathbf{u}_h) \cdot \mathbf{s} \right\|_{0,e}^2 + \|\theta_D - \theta_h\|_{0,e}^2 \right\}. \end{aligned} \quad (3.36)$$

Proof. The result follows analogously to the proof of Lemma 3.10 (see also [12, Lemma 3.8]), taking into account now the Helmholtz decomposition provided by part (b) of Lemma 3.3 and the fact that $\mathcal{R}_h(\mathbf{q}_h) = 0 \quad \forall \mathbf{q}_h \in \mathbf{H}_h^{\mathbf{P}}$ (cf (3.17)). In particular, using the alternative definition of \mathcal{R}_h (cf. (3.24)) and proceeding similarly to Lemma 3.8, we find the first, second and last term of the local estimator (3.36). On the other hand, considering the original definition (3.16) of \mathcal{R}_h , noting that $\frac{d\theta_D}{ds} \in L^2(\Gamma_D)$, applying the integration by parts formula on Γ_D given by (cf. [15, Lemma 3.5, eq. (3.34)])

$$\langle \mathbf{curl} \chi \cdot \mathbf{n}, \theta_D \rangle_{\Gamma_D} = - \left\langle \frac{d\theta_D}{ds}, \chi \right\rangle_{\Gamma_D} \quad \forall \chi \in \mathbf{H}^1(\Omega), \quad (3.37)$$

and proceeding analogously to Lemma 3.9 (see also [12, Lemma 3.7]), we obtain the remaining terms of (3.36). Further details are omitted. \square

The reliability estimate for Θ_2 is stated now.

Theorem 3.12 *Assume that the data \mathbf{f}, g and θ_D satisfy (3.21). Assume further that $\theta_D \in \mathbf{H}^1(\Gamma_D)$. Then there exist $\tilde{C}_{\text{rel}} > 0$, independent of h , such that*

$$\|(\mathbf{t}, \mathbf{u}, \mathbf{p}, \theta) - (\mathbf{t}_h, \mathbf{u}_h, \mathbf{p}_h, \theta_h)\| \leq \tilde{C}_{\text{rel}} \Theta_2. \quad (3.38)$$

Proof. It is a straightforward consequence of the definition of Θ_2 (cf. (3.6)), Lemmas 3.6, 3.10, and 3.11, and the fact that the terms $h_T^2 \|\nabla \theta_h - (\kappa^{-1} \mathbf{p}_h + \kappa^{-1} \theta_h \mathbf{u}_h)\|_{0,T}^2$ and $h_e \|\theta_D - \theta_h\|_{0,e}^2$, which form part of $\Theta_{h,T}^2$ (cf. (3.36)), are dominated by $\|\nabla \theta_h - (\kappa^{-1} \mathbf{p}_h + \kappa^{-1} \theta_h \mathbf{u}_h)\|_{0,T}^2$ and $\|\theta_D - \theta_h\|_{0,e}^2$, respectively. \square

3.5 Efficiency of the a posteriori error estimators

We now aim to establish the lower bounds in (3.8) and (3.9). For this purpose, we will make extensive use of the original system of equations given by (2.8), which is recovered from the augmented-mixed continuous formulation (2.11) by choosing suitable test functions and then integrating by parts backwardly the corresponding equations.

We begin with the efficiency estimate for Θ_1 .

Theorem 3.13 *There exists $C_{\text{eff}} > 0$, independent of h , such that*

$$C_{\text{eff}} \Theta_1 \leq \|(\mathbf{t}, \mathbf{u}, \mathbf{p}, \theta) - (\mathbf{t}_h, \mathbf{u}_h, \mathbf{p}_h, \theta_h)\|. \quad (3.39)$$

Proof. We first introduce the identity $\boldsymbol{\sigma}^d - \mu(\theta) \mathbf{t} = 0$ (cf. (2.8)), that is,

$$\boldsymbol{\sigma}_h^d - \mu(\theta_h) \mathbf{t}_h = \left(\boldsymbol{\sigma}_h^d - \boldsymbol{\sigma}^d \right) + \mu(\theta_h) (\mathbf{t} - \mathbf{t}_h) + (\mu(\theta) - \mu(\theta_h)) \mathbf{t},$$

which, proceeding as in [6, Lemma 3.4], and noting that $\|\boldsymbol{\tau}^d\|_{0,\Omega} \leq \|\boldsymbol{\tau}\|_{0,\Omega}$ for each $\boldsymbol{\tau} \in \mathbb{L}^2(\Omega)$, yields

$$\left\| \boldsymbol{\sigma}_h^d - \mu(\theta_h) \mathbf{t}_h \right\|_{0,\Omega}^2 \leq 3 \left\{ \mu_2^2 \|\mathbf{t} - \mathbf{t}_h\|_{0,\Omega}^2 + \|\boldsymbol{\sigma} - \boldsymbol{\sigma}_h\|_{0,\Omega}^2 + L_\mu^2 \|\mathbf{t}\|_{\delta,\Omega}^2 \|\theta - \theta_h\|_{L^{n/\delta}(\Omega)}^2 \right\}.$$

Recall here from [6] that $\delta \in (0, 1)$ (when $n = 2$) or $\delta \in (1/2, 1)$ (when $n = 3$) stands for the extra regularity that we need to assume for the solution of (2.11). In turn, employing the estimate [6, eq. (3.22)] to bound $\|\mathbf{t}\|_{\delta,\Omega}$, and the continuous injection of $H^1(\Omega)$ into $L^{n/\delta}(\Omega)$, whose boundedness constant is \tilde{C}_δ (cf. Theorem 2.1), it is not difficult to see that there exist a positive constant c_1 , depending only on data and other constants, all of them independent of h , such that

$$\left\| \boldsymbol{\sigma}_h^d - \mu(\theta_h) \mathbf{t}_h \right\|_{0,\Omega}^2 \leq c_1 \left\{ \|\mathbf{t} - \mathbf{t}_h\|_{0,\Omega}^2 + \|\boldsymbol{\sigma} - \boldsymbol{\sigma}_h\|_{0,\Omega}^2 + \|\theta - \theta_h\|_{1,\Omega}^2 \right\}. \quad (3.40)$$

Analogously, by considering the identity $\nabla \theta - (\kappa^{-1} \mathbf{p} + \kappa^{-1} \theta \mathbf{u}) = 0$ (cf. (2.8)), we have

$$\nabla \theta_h - (\kappa^{-1} \mathbf{p}_h + \kappa^{-1} \theta_h \mathbf{u}_h) = \nabla(\theta_h - \theta) + \kappa^{-1}(\mathbf{p} - \mathbf{p}_h) + \kappa^{-1}(\theta \mathbf{u} - \theta_h \mathbf{u}_h),$$

where the last term of the right-hand side can be rewritten as $\theta \mathbf{u} - \theta_h \mathbf{u}_h = \theta(\mathbf{u} - \mathbf{u}_h) + (\theta - \theta_h) \mathbf{u}_h$, and then it can be bounded by

$$\|\theta \mathbf{u} - \theta_h \mathbf{u}_h\|_{0,\Omega} \leq \|\theta\|_{L^4(\Omega)} \|\mathbf{u} - \mathbf{u}_h\|_{L^4(\Omega)} + \|\mathbf{u}_h\|_{L^4(\Omega)} \|\theta - \theta_h\|_{L^4(\Omega)}.$$

Therefore, using the fact that $H^1(\Omega)$ is continuously embedded into $L^4(\Omega)$, θ lives in the ball \mathcal{W} , and the estimate $\|\mathbf{u}_h\|_{1,\Omega} \leq c_S \|\mathbf{f}\|_{0,\Omega}$ holds (cf. (2.22)), we obtain

$$\|\nabla \theta_h - (\kappa^{-1} \mathbf{p}_h + \kappa^{-1} \theta_h \mathbf{u}_h)\|_{0,\Omega}^2 \leq c_2 \|(\mathbf{u}, \mathbf{p}, \theta) - (\mathbf{u}_h, \mathbf{p}_h, \theta_h)\|^2, \quad (3.41)$$

with c_2 a positive constant independent of h . On the other hand, it is readily seen from (2.8) that

$$\begin{aligned}
\|\mathbf{f} + \mathbf{div} \boldsymbol{\sigma}_h\|_{0,\Omega}^2 &\leq \|\mathbf{div} (\boldsymbol{\sigma} - \boldsymbol{\sigma}_h)\|_{0,\Omega}^2, \\
\|g + \mathbf{div} \mathbf{p}_h\|_{0,\Omega}^2 &\leq \|\mathbf{div} (\mathbf{p} - \mathbf{p}_h)\|_{0,\Omega}^2, \\
\|\boldsymbol{\sigma}_h - \boldsymbol{\sigma}_h^t\|_{0,\Omega}^2 &\leq 4\|\boldsymbol{\sigma} - \boldsymbol{\sigma}_h\|_{0,\Omega}^2, \\
\|\mathbf{t}_h - \mathbf{e}(\mathbf{u}_h)\|_{0,\Omega}^2 &\leq 2\left\{\|\mathbf{t} - \mathbf{t}_h\|_{0,\Omega}^2 + \|\mathbf{u} - \mathbf{u}_h\|_{1,\Omega}^2\right\}, \\
\|\boldsymbol{\rho}_h - (\nabla \mathbf{u}_h - \mathbf{e}(\mathbf{u}_h))\|_{0,\Omega}^2 &\leq 2\left\{\|\boldsymbol{\rho} - \boldsymbol{\rho}_h\|_{0,\Omega}^2 + \|\mathbf{u} - \mathbf{u}_h\|_{1,\Omega}^2\right\}, \\
\|\nabla \mathbf{u}_h - (\mathbf{t}_h + \boldsymbol{\rho}_h)\|_{0,\Omega}^2 &\leq 3\left\{\|\mathbf{t} - \mathbf{t}_h\|_{0,\Omega}^2 + \|\boldsymbol{\rho} - \boldsymbol{\rho}_h\|_{0,\Omega}^2 + \|\mathbf{u} - \mathbf{u}_h\|_{1,\Omega}^2\right\}, \\
\|\theta_D - \theta_h\|_{0,\Gamma_D}^2 &\leq c_3\|\theta - \theta_h\|_{1,\Omega}^2,
\end{aligned} \tag{3.42}$$

and

$$\|\theta_D - \theta_h\|_{1/2,\Gamma_D}^2 \leq c_4\|\theta - \theta_h\|_{1,\Omega}^2, \tag{3.43}$$

where the last two inequalities make use of the trace inequalities in $L^2(\Gamma_D)$ and $H^{1/2}(\Gamma_D)$, respectively. In this way, the required efficiency estimate (3.39) follows straightforwardly from the definition of Θ_1 (cf. (3.5)) and the inequalities (3.40)–(3.43). \square

Next, we continue with the derivation of the efficiency estimate of Θ_2 .

Lemma 3.14 *There hold*

- (a) $\|\mathbf{f} - \mathbf{P}_h(\mathbf{f})\|_{0,T} \leq 2\|\mathbf{div} (\boldsymbol{\sigma} - \boldsymbol{\sigma}_h)\|_{0,T} \quad \forall T \in \mathcal{T}_h,$
- (b) $\|g - \mathcal{P}_h(g)\|_{0,T} \leq 2\|\mathbf{div} (\mathbf{p} - \mathbf{p}_h)\|_{0,T} \quad \forall T \in \mathcal{T}_h,$

and there exist $c_1, c_2 > 0$, independent of h , such that

- (c) $h_T^2 \|\mathbf{rot} (\mathbf{t}_h + \boldsymbol{\rho}_h)\|_{0,T}^2 \leq c_1 \left\{ \|\mathbf{t} - \mathbf{t}_h\|_{0,T}^2 + \|\boldsymbol{\rho} - \boldsymbol{\rho}_h\|_{0,T}^2 \right\} \quad \forall T \in \mathcal{T}_h,$
- (d) $h_e \|\llbracket (\mathbf{t}_h + \boldsymbol{\rho}_h) \mathbf{s} \rrbracket\|_{0,e}^2 \leq c_2 \left\{ \|\mathbf{t} - \mathbf{t}_h\|_{0,\omega_e}^2 + \|\boldsymbol{\rho} - \boldsymbol{\rho}_h\|_{0,\omega_e}^2 \right\} \quad \forall e \in \mathcal{E}_h,$

where the set ω_e is given by $\omega_e := \cup\{T' \in \mathcal{T}_h : e \in \mathcal{E}(T')\}$.

Proof. For (a) and (b) we refer to [25, Lemma 3.18]. In turn, since $\mathbf{rot} (\mathbf{t} + \boldsymbol{\rho}) = \mathbf{rot} (\nabla \mathbf{u}) = \mathbf{0}$, we find that the proof of (c) and (d) follows after a straightforward application of [3, Lemmas 4.3 and 4.4], respectively. \square

The corresponding bounds for the remaining terms defining Θ_2 are given next.

Lemma 3.15 *There exist $c_1, c_2 > 0$, independent of h , such that*

- (a) $\sum_{T \in \mathcal{T}_h} h_T^2 \|\mathbf{rot} (\kappa^{-1} \mathbf{p}_h + \kappa^{-1} \theta_h \mathbf{u}_h)\|_{0,T}^2 \leq c_1 \|(\mathbf{u}, \mathbf{p}, \theta) - (\mathbf{u}_h, \mathbf{p}_h, \theta_h)\|^2,$
- (b) $\sum_{e \in \mathcal{E}_h(\Omega)} h_e \|\llbracket (\kappa^{-1} \mathbf{p}_h + \kappa^{-1} \theta_h \mathbf{u}_h) \cdot \mathbf{s} \rrbracket\|_{0,e}^2 \leq c_2 \|(\mathbf{u}, \mathbf{p}, \theta) - (\mathbf{u}_h, \mathbf{p}_h, \theta_h)\|^2.$

In addition, under the assumption that $\theta_D \in H^1(\Gamma_D)$, there exists $c_3 > 0$, independent of h , such that

$$(c) \quad \sum_{e \in \mathcal{E}_h(\Gamma_D)} h_e \left\| \frac{d\theta_D}{ds} - (\kappa^{-1} \mathbf{p}_h + \kappa^{-1} \theta_h \mathbf{u}_h) \cdot \mathbf{s} \right\|_{0,e}^2 \leq c_3 \|(\mathbf{u}, \mathbf{p}, \theta) - (\mathbf{u}_h, \mathbf{p}_h, \theta_h)\|^2.$$

Proof. It follows almost straightforwardly from a slight modification of the proof of [12, Lemma 3.11]. We omit further details. \square

As a consequence of Theorem 3.13 and Lemmas 3.14 and 3.15, we are now in position to state the efficiency of Θ_2 .

Theorem 3.16 *Assume that $\theta_D \in H^1(\Gamma_D)$. Then, there exists $\tilde{C}_{\text{eff}} > 0$, independent of h , such that*

$$\tilde{C}_{\text{eff}} \Theta_2 \leq \|(\underline{\mathbf{t}}, \mathbf{u}, \mathbf{p}, \theta) - (\underline{\mathbf{t}}_h, \mathbf{u}_h, \mathbf{p}_h, \theta_h)\|. \quad (3.44)$$

4 A posteriori error analysis: the 3D-case

In this section we extend the results from Section 3 to the three-dimensional version of (2.21). Similarly as in the previous section, given a tetrahedron $T \in \mathcal{T}_h$, we let $\mathcal{E}(T)$ be the set of its faces, and let \mathcal{E}_h be the set of all faces of the triangulation \mathcal{T}_h . Then, we write $\mathcal{E}_h = \mathcal{E}_h(\Omega) \cup \mathcal{E}_h(\Gamma_D) \cup \mathcal{E}_h(\Gamma_N)$, where $\mathcal{E}_h(\Omega) := \{e \in \mathcal{E}_h : e \subseteq \Omega\}$, $\mathcal{E}_h(\Gamma_D) := \{e \in \mathcal{E}_h : e \subseteq \Gamma_D\}$, and $\mathcal{E}_h(\Gamma_N) := \{e \in \mathcal{E}_h : e \subseteq \Gamma_N\}$. Also, for each face $e \in \mathcal{E}_h$ we fix a unit normal \mathbf{n}_e to e , so that given $\boldsymbol{\tau} \in \mathbb{L}^2(\Omega)$ such that $\boldsymbol{\tau}|_T \in \mathbb{C}(T)$ on each $T \in \mathcal{T}_h$, and given $e \in \mathcal{E}_h(\Omega)$, we let $\llbracket \boldsymbol{\tau} \times \mathbf{n}_e \rrbracket$ be the corresponding jump of the tangential traces across e , that is $\llbracket \boldsymbol{\tau} \times \mathbf{n}_e \rrbracket := (\boldsymbol{\tau}|_T - \boldsymbol{\tau}|_{T'})|_e \times \mathbf{n}_e$, where T and T' are the elements of \mathcal{T}_h having e as a common face. In what follows, when no confusion arises, we simply write \mathbf{n} instead of \mathbf{n}_e .

Now, we recall that the curl of a 3D vector $\mathbf{v} := (v_1, v_2, v_3)$ is the 3D vector

$$\text{curl}(\mathbf{v}) = \nabla \times \mathbf{v} := \left(\frac{\partial v_3}{\partial x_2} - \frac{\partial v_2}{\partial x_3}, \frac{\partial v_1}{\partial x_3} - \frac{\partial v_3}{\partial x_1}, \frac{\partial v_2}{\partial x_1} - \frac{\partial v_1}{\partial x_2} \right),$$

and that, given a tensor function $\boldsymbol{\tau} := (\tau_{ij})_{3 \times 3}$, the operator $\underline{\text{curl}}(\boldsymbol{\tau})$ is the 3×3 tensor whose rows are given by

$$\underline{\text{curl}}(\boldsymbol{\tau}) := \begin{pmatrix} \text{curl}(\tau_{11}, \tau_{12}, \tau_{13}) \\ \text{curl}(\tau_{21}, \tau_{22}, \tau_{23}) \\ \text{curl}(\tau_{31}, \tau_{32}, \tau_{33}) \end{pmatrix}.$$

In addition, $\boldsymbol{\tau} \times \mathbf{n}$ stands for the 3×3 tensor whose rows are given by the tangential components of each row of $\boldsymbol{\tau}$, that is,

$$\boldsymbol{\tau} \times \mathbf{n} := \begin{pmatrix} (\tau_{11}, \tau_{12}, \tau_{13}) \times \mathbf{n} \\ (\tau_{21}, \tau_{22}, \tau_{23}) \times \mathbf{n} \\ (\tau_{31}, \tau_{32}, \tau_{33}) \times \mathbf{n} \end{pmatrix}.$$

Having introduced these notations, we now set for each $T \in \mathcal{T}_h$ the local a posteriori error indicators $\tilde{\Theta}_{1,T}^2$ and $\Theta_{1,T}^2$ (exactly as in (3.4) and (3.5), respectively), and define

$$\begin{aligned} \Theta_{2,T}^2 &:= \tilde{\Theta}_{1,T}^2 + \|\mathbf{f} - \mathbf{P}_h(\mathbf{f})\|_{0,T}^2 + \|g - \mathcal{P}_h(g)\|_{0,T}^2 + h_T^2 \|\nabla \mathbf{u}_h - (\mathbf{t}_h + \boldsymbol{\rho}_h)\|_{0,T}^2 \\ &+ h_T^2 \|\underline{\text{curl}}(\mathbf{t}_h + \boldsymbol{\rho}_h)\|_{0,T}^2 + h_T^2 \|\text{curl}(\kappa^{-1} \mathbf{p}_h + \kappa^{-1} \theta_h \mathbf{u}_h)\|_{0,T}^2 \\ &+ \sum_{e \in \mathcal{E}(T)} h_e \|\llbracket (\mathbf{t}_h + \boldsymbol{\rho}_h) \times \mathbf{n} \rrbracket\|_{0,e}^2 + \sum_{e \in \mathcal{E}(T) \cap \mathcal{E}_h(\Omega)} h_e \|\llbracket (\kappa^{-1} \mathbf{p}_h + \kappa^{-1} \theta_h \mathbf{u}_h) \times \mathbf{n} \rrbracket\|_{0,e}^2 \\ &+ \sum_{e \in \mathcal{E}(T) \cap \mathcal{E}_h(\Gamma_D)} h_e \|\nabla \theta_D \times \mathbf{n} - (\kappa^{-1} \mathbf{p}_h + \kappa^{-1} \theta_h \mathbf{u}_h) \times \mathbf{n}\|_{0,e}^2. \end{aligned} \quad (4.1)$$

In this way, the corresponding global a posteriori error estimators are defined as in (3.7), that is

$$\Theta_1 := \left\{ \sum_{T \in \mathcal{T}_h} \Theta_{1,T}^2 + \|\theta_D - \theta_h\|_{1/2, \Gamma_D}^2 \right\}^{1/2} \quad \text{and} \quad \Theta_2 := \left\{ \sum_{T \in \mathcal{T}_h} \Theta_{2,T}^2 \right\}^{1/2},$$

and the main estimates, which are the analogue of Theorems 3.7 and 3.12, are as follows.

Theorem 4.1 *Assume that the data \mathbf{f}, g and θ_D satisfy (3.21). Assume further that $\theta_D \in \mathbf{H}^1(\Gamma_D)$. Then, there exist positive constants $C_{\text{rel}}, C_{\text{eff}}, \tilde{C}_{\text{rel}}$, and \tilde{C}_{eff} , independent of h , such that*

$$C_{\text{eff}} \Theta_1 \leq \|(\mathbf{t}, \mathbf{u}, \mathbf{p}, \theta) - (\mathbf{t}_h, \mathbf{u}_h, \mathbf{p}_h, \theta_h)\| \leq C_{\text{rel}} \Theta_1$$

and

$$\tilde{C}_{\text{eff}} \Theta_2 \leq \|(\mathbf{t}, \mathbf{u}, \mathbf{p}, \theta) - (\mathbf{t}_h, \mathbf{u}_h, \mathbf{p}_h, \theta_h)\| \leq \tilde{C}_{\text{rel}} \Theta_2.$$

The proof of Theorem 4.1 follows very closely the analysis of Section 3, except a few issues to be described throughout the following discussion. Indeed, we first observe that the general a posteriori error estimate given by Lemma 3.6 is also valid in 3D, and that the corresponding upper bounds of $\|\mathcal{R}_f\|_{\mathbb{H}_0(\text{div}; \Omega)'} and $\|\mathcal{R}_h\|_{\mathbf{H}_{\Gamma_N}(\text{div}; \Omega)'}$ yielding the reliability of Θ_1 are the same as those given in (3.26) and (3.27), respectively.$

Now, for the reliability of Θ_2 , we need to use a 3D version of the stable Helmholtz decompositions provided by Lemma 3.3. These required results were established recently for arbitrary polyhedral domains in [22, Theorems 3.1 and 3.2]. Next, the associated discrete Helmholtz decompositions and the functionals \mathcal{R}_f and \mathcal{R}_h are set and rewritten exactly as in (3.23) and (3.24), respectively. Furthermore, in order to derive the new upper bound of $\|\mathcal{R}_f\|_{\mathbb{H}_0(\text{div}; \Omega)'}$ and $\|\mathcal{R}_h\|_{\mathbf{H}_{\Gamma_N}(\text{div}; \Omega)'}$, we now need the 3D analogue of the integration by parts formula on the boundary given by (3.37). In fact, by applying the identities from [26, Chapter I, eq. (2.17) and Theorem 2.11], we deduce that in this case there holds

$$\langle \text{curl } \boldsymbol{\chi} \cdot \mathbf{n}, \theta_D \rangle_{\Gamma_D} = - \langle \nabla \theta_D \times \mathbf{n}, \boldsymbol{\chi} \rangle_{\Gamma_D} \quad \forall \boldsymbol{\chi} \in \mathbf{H}^1(\Omega).$$

In addition, the integration by parts formula on each tetrahedron $T \in \mathcal{T}_h$, which is employed in the proof of the 3D analogue of Lemma 3.9, becomes (cf. [26, Chapter I, Theorem 2.11])

$$\int_T \text{curl } \mathbf{q} \cdot \boldsymbol{\chi} - \int_T \mathbf{q} \cdot \text{curl } \boldsymbol{\chi} = \langle \mathbf{q} \times \mathbf{n}, \boldsymbol{\chi} \rangle_{\partial T} \quad \forall \mathbf{q} \in \mathbf{H}(\text{curl}; \Omega), \quad \forall \boldsymbol{\chi} \in \mathbf{H}^1(\Omega),$$

where $\langle \cdot, \cdot \rangle_{\partial T}$ is the duality pairing between $\mathbf{H}^{-1/2}(\partial T)$ and $\mathbf{H}^{1/2}(\partial T)$, and, as usual, $\mathbf{H}(\text{curl}; \Omega)$ is the space of vectors in $\mathbf{L}^2(\Omega)$ whose curl lie also in $\mathbf{L}^2(\Omega)$. Note that the foregoing identities explain the appearing of the expressions $(\mathbf{t}_h + \boldsymbol{\rho}_h) \times \mathbf{n}$, $(\kappa^{-1} \mathbf{p}_h + \kappa^{-1} \theta_h \mathbf{u}_h) \times \mathbf{n}$, and $\nabla \theta_D \times \mathbf{n} - (\kappa^{-1} \mathbf{p}_h + \kappa^{-1} \theta_h \mathbf{u}_h) \times \mathbf{n}$ in the 3D definitions of $\Theta_{2,T}^2$ (cf. (4.1)). The rest of the proof of the reliability of Θ_2 and the entire analysis yielding the efficiency of both Θ_1 and Θ_2 proceed as in Sections 3.4 and 3.5, respectively, taking into account that the proof of the 3D version of the Lemma 3.15 follows almost straightforwardly from a slight modification of the proof of [12, Lemma 4.2].

5 Numerical results

This section serves to illustrate the performance and accuracy of the proposed augmented finite element scheme along with the properties of the a posteriori error estimators Θ_1 and Θ_2 , in 2D and 3D domains,

derived in Sections 3 and 4, respectively. In this regard, we remark that for purposes of adaptivity, which requires to have locally computable indicators, we use that

$$\|\theta_D - \theta_h\|_{1/2, \Gamma_D}^2 \leq c_D \|\theta_D - \theta_h\|_{1, \Gamma_D}^2 = c_D \sum_{e \in \mathcal{E}_h(\Gamma_D)} \|\theta_D - \theta_h\|_{1, e}^2,$$

and redefine Θ_1 as

$$\Theta_1 := \left\{ \sum_{T \in \mathcal{T}_h} \Theta_{1, T}^2 \right\}^{1/2},$$

where

$$\begin{aligned} \Theta_{1, T}^2 := & \left\| \boldsymbol{\sigma}_h^d - \mu(\theta_h) \mathbf{t}_h \right\|_{0, T}^2 + \|\mathbf{f} + \mathbf{div} \boldsymbol{\sigma}_h\|_{0, T}^2 + \|\boldsymbol{\sigma}_h - \boldsymbol{\sigma}_h^t\|_{0, T}^2 + \|\mathbf{t}_h - \mathbf{e}(\mathbf{u}_h)\|_{0, T}^2 \\ & + \|\boldsymbol{\rho}_h - (\nabla \mathbf{u}_h - \mathbf{e}(\mathbf{u}_h))\|_{0, T}^2 + \|\nabla \mathbf{u}_h - (\mathbf{t}_h + \boldsymbol{\rho}_h)\|_{0, T}^2 + \|g + \mathbf{div} \mathbf{p}_h\|_{0, T}^2 \\ & + \|\nabla \theta_h - (\kappa^{-1} \mathbf{p}_h + \kappa^{-1} \theta_h \mathbf{u}_h)\|_{0, T}^2 + \sum_{e \in \mathcal{E}(T) \cap \mathcal{E}_h(\Gamma_D)} \|\theta_D - \theta_h\|_{1, e}^2. \end{aligned}$$

Under this redefinition Θ_1 is certainly still reliable, but efficient only up to all its terms, except for the last one, associated to the boundary Γ_D . Nevertheless, the numerical results to be displayed below allow us to conjecture that this modified Θ_1 actually verifies both properties.

Our implementation is based on the public domain finite element software `FreeFem++` [27] which provides for both 2D and 3D domains the automatic adaptation procedure tools `adaptmesh` and `msh-met`, respectively. A Picard algorithm with a fixed tolerance `tol = 1E - 6` has been used for the corresponding fixed-point problem (2.21) and the iterations are terminated once the relative error of the entire coefficient vectors between two consecutive iterates is sufficiently small, i.e.,

$$\frac{\|\text{coeff}^{m+1} - \text{coeff}^m\|_{l^2}}{\|\text{coeff}^{m+1}\|_{l^2}} \leq \text{tol},$$

where $\|\cdot\|_{l^2}$ is the standard l^2 -norm in \mathbb{R}^N , with N denoting the total number of degrees of freedom defining the finite element subspaces $\mathbb{H}_h^t, \mathbb{H}_h^\sigma, \mathbb{H}_h^\rho, \mathbf{H}_h^u, \mathbf{H}_h^p$, and H_h^θ . As usual, the individual errors are denoted by:

$$\begin{aligned} \mathbf{e}(\mathbf{t}) &:= \|\mathbf{t} - \mathbf{t}_h\|_{0, \Omega}, & \mathbf{e}(\boldsymbol{\sigma}) &:= \|\boldsymbol{\sigma} - \boldsymbol{\sigma}_h\|_{\text{div}; \Omega}, & \mathbf{e}(\boldsymbol{\rho}) &:= \|\boldsymbol{\rho} - \boldsymbol{\rho}_h\|_{0, \Omega}, \\ \mathbf{e}(\mathbf{u}) &:= \|\mathbf{u} - \mathbf{u}_h\|_{1, \Omega}, & \mathbf{e}(\mathbf{p}) &:= \|\mathbf{p} - \mathbf{p}_h\|_{\text{div}; \Omega}, & \mathbf{e}(\theta) &:= \|\theta - \theta_h\|_{1, \Omega}, \\ \mathbf{e}(\boldsymbol{\sigma}_P) &:= \|\boldsymbol{\sigma}_P - \boldsymbol{\sigma}_{P, h}\|_{0, \Omega}, & \mathbf{e}(p) &:= \|p - p_h\|_{0, \Omega}, \end{aligned}$$

where $\boldsymbol{\sigma}_{P, h}$ and p_h , are the postprocessed polymeric part of the extra-stress tensor and the pressure, respectively, given by

$$\boldsymbol{\sigma}_{P, h} := 2\mu_P(\theta_h) \mathbf{t}_h \quad \text{and} \quad p_h := -\frac{1}{n} \text{tr} \boldsymbol{\sigma}_h \quad \text{in} \quad \Omega.$$

In turn, the global error is computed as

$$\mathbf{e} := \left\{ \mathbf{e}(\mathbf{t})^2 + \mathbf{e}(\boldsymbol{\sigma})^2 + \mathbf{e}(\boldsymbol{\rho})^2 + \mathbf{e}(\mathbf{u})^2 + \mathbf{e}(\mathbf{p})^2 + \mathbf{e}(\theta)^2 \right\}^{1/2},$$

whereas the effectivity index with respect to Θ_i , $i \in \{1, 2\}$ is given by

$$\text{eff}(\Theta_i) := \frac{e}{\Theta_i}.$$

In addition, we define the experimental rates of convergence

$$r(\diamond) := \frac{\log(e(\diamond)/e'(\diamond))}{\log(h/h')} \quad \text{for each } \diamond \in \{\mathbf{t}, \boldsymbol{\sigma}, \boldsymbol{\rho}, \mathbf{u}, \mathbf{p}, \theta, \boldsymbol{\sigma}_P, p\},$$

where e and e' denote errors computed on two consecutive meshes of sizes h and h' , respectively. However, when the adaptive algorithm is applied, the expression $\log(h/h')$ appearing in the computation of the above rates is replaced by $-\frac{1}{n} \log(N/N')$ with $n = 2$ (in 2D domains) or $n = 3$ (in 3D domains), where N and N' denote the corresponding degrees of freedom of each triangulation.

The examples to be considered in this section are described next. In all of them, as in [13, Section 2], we choose the coefficients of the polymer and solvent viscosity a_1, b_1, a_2 and b_2 (cf. (2.2)) as follow:

$$b_1 = b_2 = \frac{\Delta E}{R}, \quad a_2 = \exp\left(\frac{-\Delta E}{R\theta_R}\right), \quad \text{and} \quad a_1 = (1 - \epsilon)a_2,$$

where ΔE is the activation energy, R is the ideal gas constant, and θ_R is a reference temperature of the fluid. Note that the constraint (2.3) will be satisfied as long as the temperature of the system stays above θ_R . In turn, we consider $\kappa = 1$, $\epsilon = 0.01$, and according to [6, eq. (3.20)], the stabilization parameters are taken as $\kappa_1 = \mu_1/\mu_2^2$, $\kappa_2 = \kappa_1$, $\kappa_3 = \mu_1/2$, $\kappa_4 = \mu_1/4$, $\kappa_5 = \kappa$, $\kappa_6 = \kappa^{-1}/2$, and $\kappa_7 = \kappa/2$. In addition, the condition $\int_{\Omega} \text{tr } \boldsymbol{\sigma}_h = 0$ is imposed via a penalization strategy.

Example 1. In our first example we concentrate on the accuracy of the augmented method. We consider the square domain $\Omega := (0, 1)^2$, the boundary $\Gamma = \bar{\Gamma}_D \cup \bar{\Gamma}_N$, with $\Gamma_D := \{0\} \times (0, 1)$ and $\Gamma_N := \Gamma \setminus \bar{\Gamma}_D$. The following viscosity parameters correspond to polystyrene [28, Section 4.2]:

$$\frac{\Delta E}{R} = 14500, \quad \theta_R = 538.$$

The data \mathbf{f} , g , and θ_D are chosen so that a manufactured solution of (2.8) is given by the smooth functions

$$\begin{aligned} \mathbf{u}(\mathbf{x}) &:= \begin{pmatrix} 2\pi x_1^2(x_1 - 1)^2 \cos(\pi x_2) \sin(\pi x_2) \\ -2x_1(x_1 - 1)(2x_1 - 1) \sin(\pi x_2)^2 \end{pmatrix}, \\ p(\mathbf{x}) &:= \cos(\pi x_1) \cos(\pi x_2), \\ \theta(\mathbf{x}) &:= 10(x_1 - 1)^2 \sin(\pi x_2)^2 + 540 \quad \forall \mathbf{x} := (x_1, x_2) \in \Omega. \end{aligned}$$

The results reported in Tables 5.1 and 5.2 are in accordance with the theoretical bounds established in Theorem 2.2. In addition, we also compute the global a posteriori error indicators Θ_1, Θ_2 and measure their reliability and efficiency with the effectivity index. For the two orders tested, these estimators remain always bounded.

Example 2. Our second example is aimed at testing the features of adaptive mesh refinement after the a posteriori error estimators Θ_1 and Θ_2 . We consider a four-to-one contraction domain $\Omega := (0, 2) \times (0, 1) \setminus (1, 2) \times (0.25, 1)$, the boundary $\Gamma = \bar{\Gamma}_D \cup \bar{\Gamma}_N$, with $\Gamma_D := \{0\} \times (0, 1)$ and $\Gamma_N := \Gamma \setminus \bar{\Gamma}_D$. The following viscosity parameters correspond to Nylon-6,6 [28, Section 4.2]:

$$\frac{\Delta E}{R} = 6600, \quad \theta_R = 563.$$

The data \mathbf{f} , g , and θ_D are chosen so that the exact solution is given by

$$\begin{aligned}\mathbf{u}(\mathbf{x}) &:= \begin{pmatrix} x_2(x_2 - 1)(x_2 - 0.25)(3x_2^2 - 2.5x_2 + 0.25) \sin(\pi x_1)^2 \\ -\pi x_2^2(x_2 - 1)^2(x_2 - 0.25)^2 \cos(\pi x_1) \sin(\pi x_1) \end{pmatrix}, \\ p(\mathbf{x}) &:= \frac{10(x_2 - 0.25)}{(x_1 - 1.02)^2 + (x_2 - 0.27)^2} + p_0, \\ \theta(\mathbf{x}) &:= \frac{4(x_1 - 1)(x_2 - 0.25)}{(x_1 - 1.02)^2 + (x_2 - 0.27)^2} + 570 \quad \forall \mathbf{x} := (x_1, x_2) \in \Omega.\end{aligned}$$

The constant p_0 is such that $\int_{\Omega} p = 0$. Notice that both the pressure and the temperature exhibit high gradients near the vertex $(1, 0.25)$. Notice also that the only difference with respect to (2.8) is a non-homogeneous heat flux $\mathbf{p} \cdot \mathbf{n} = f_N$ imposed on Γ_N , where f_N is manufactured according to the above solution. Therefore, the local estimators $\Theta_{1,T}$ and $\Theta_{2,T}$ have to be modified by adding the term

$$\sum_{e \in \mathcal{E}(T) \cap \mathcal{E}_h(\Gamma_N)} h_e \|f_N - \mathbf{p}_h \cdot \mathbf{n}\|_{0,e}^2,$$

whose estimation from below and above follows in a straightforward manner.

Tables 5.3, 5.4, and 5.5 along with Figure 5.1, summarizes the convergence history of the method applied to a sequence of quasi-uniformly and adaptively refined triangulation of the domain. Sub-optimal rates are observed in the first case, whereas adaptive refinement according to either a posteriori error indicator yield optimal convergence and stable effectivity indexes. On the other hand, approximate solutions builded using the augmented $\mathbb{P}_0 - \mathbb{RT}_0 - \mathbb{P}_0 - \mathbf{P}_1 - \mathbf{RT}_0 - \mathbf{P}_1$ scheme with 562743 degrees of freedom (via the indicator Θ_1) are shown in Figure 5.2. In particular, we observe in both the velocity and heat flux streamlines a vortex near the corner region of the four-to-one domain whereas both the pressure and temperature exhibit high gradients in the same region. In turn, examples of some adapted meshes generated using Θ_1 and Θ_2 are collected in Figure 5.3. We can observe a clear clustering of elements near the corner region of the contraction as we expected. Notice that the meshes obtained via the indicator Θ_2 are lightly more refined in the interior of the contraction domain than the meshes obtained via the indicator Θ_1 . This fact is justified by the terms that capture the jumps between triangles obtained in the Helmholtz decomposition.

Example 3. To conclude, we replicate the Example 2 in a three-dimensional setting. In fact, we consider the four-to-one domain $\Omega := (0, 2) \times (0, 1)^2 \setminus (1, 2) \times (0.25, 1)^2$, the boundary $\Gamma = \bar{\Gamma}_D \cup \bar{\Gamma}_N$, with $\Gamma_D := \{0\} \times (0, 1)^2$ and $\Gamma_N := \Gamma \setminus \bar{\Gamma}_D$. The viscosity parameters are the same as in the second example. However, this time the manufactured exact solutions adopt the form

$$\begin{aligned}\mathbf{u}(\mathbf{x}) &:= \begin{pmatrix} -x_3(x_3 - 1)(x_3 - 0.25)(3x_3^2 - 2.5x_3 - \pi \cos(\pi x_2) + 0.25) \sin(\pi x_1)^2 \sin(\pi x_2) \\ x_3(x_3 - 1)(x_3 - 0.25)(3x_3^2 - 2.5x_3 - \pi \cos(\pi x_1) + 0.25) \sin(\pi x_1) \sin(\pi x_2)^2 \\ -\pi x_3^2(x_3 - 1)^2(x_3 - 0.25)^2 \sin(\pi x_1) \sin(\pi x_2)(\cos(\pi x_2) - \cos(\pi x_1)) \end{pmatrix}, \\ p(\mathbf{x}) &:= \frac{10(x_3 - 0.25)}{(x_1 - 1.05)^2 + (x_3 - 0.3)^2} + p_0, \\ \theta(\mathbf{x}) &:= \frac{4(x_1 - 1)(x_3 - 0.25)}{(x_1 - 1.05)^2 + (x_3 - 0.3)^2} + 570 \quad \forall \mathbf{x} := (x_1, x_2, x_3) \in \Omega.\end{aligned}$$

Similarly, Tables 5.6 and 5.7 along with the Figure 5.4 confirm a disturbed convergence under quasi-uniform refinement and an optimal convergence rates when using adaptive refinement guided by the a posteriori error estimator Θ_1 . In turn, some approximated solutions after four mesh refinement steps showing an analogous behaviour to its 2D counterpart are collected in Figure 5.5, whereas snapshots of the last three meshes via Θ_1 are shown in Figure 5.6.

N	h	$e(\mathbf{t})$	$r(\mathbf{t})$	$e(\boldsymbol{\sigma})$	$r(\boldsymbol{\sigma})$	$e(\boldsymbol{\rho})$	$r(\boldsymbol{\rho})$	$e(\mathbf{u})$	$r(\mathbf{u})$	$e(p)$	$r(p)$
1467	0.196	0.155	–	1.246	–	0.268	–	0.264	–	0.148	–
5631	0.097	0.075	1.025	0.633	0.960	0.146	0.859	0.127	1.040	0.063	1.214
22131	0.048	0.038	0.979	0.310	1.009	0.080	0.858	0.062	1.018	0.031	0.995
87837	0.025	0.019	1.032	0.157	1.018	0.040	1.045	0.031	1.027	0.015	1.105
353853	0.013	0.009	1.093	0.077	1.085	0.020	1.089	0.015	1.072	0.007	1.111

$e(\mathbf{p})$	$r(\mathbf{p})$	$e(\theta)$	$r(\theta)$	$e(\boldsymbol{\sigma}_P)$	$r(\boldsymbol{\sigma}_P)$	e	r	$\text{eff}(\Theta_1)$	$\text{eff}(\Theta_2)$	iter
18.678	–	3.265	–	0.349	–	19.007	–	0.931	0.183	4
9.628	0.940	1.419	1.181	0.171	1.017	9.755	0.992	0.942	0.180	4
4.738	1.002	0.654	1.094	0.082	1.027	4.794	1.038	0.947	0.178	3
2.405	1.014	0.331	1.019	0.041	1.035	2.434	0.984	0.950	0.176	3
1.187	1.082	0.163	1.087	0.020	1.117	1.201	1.013	0.950	0.176	3

Table 5.1: EXAMPLE 1, $\mathbb{P}_0 - \mathbb{RT}_0 - \mathbb{P}_0 - \mathbf{P}_1 - \mathbf{RT}_0 - \mathbf{P}_1$ scheme with quasi-uniform refinement.

N	h	$e(\mathbf{t})$	$r(\mathbf{t})$	$e(\boldsymbol{\sigma})$	$r(\boldsymbol{\sigma})$	$e(\boldsymbol{\rho})$	$r(\boldsymbol{\rho})$	$e(\mathbf{u})$	$r(\mathbf{u})$	$e(p)$	$r(p)$
3666	0.196	0.026	–	0.151	–	0.023	–	0.037	–	0.016	–
14076	0.097	0.006	2.036	0.037	2.002	0.006	1.986	0.009	2.071	0.004	1.894
55326	0.048	0.001	2.044	0.009	2.019	0.001	2.048	0.002	2.065	0.001	1.998
219591	0.025	0.000	1.989	0.002	2.040	0.000	1.998	0.001	1.986	0.000	2.032
884631	0.013	0.000	2.186	0.000	2.153	0.000	2.196	0.000	2.195	0.000	2.167

$e(\mathbf{p})$	$r(\mathbf{p})$	$e(\theta)$	$r(\theta)$	$e(\boldsymbol{\sigma}_P)$	$r(\boldsymbol{\sigma}_P)$	e	r	$\text{eff}(\Theta_1)$	$\text{eff}(\Theta_2)$	iter
2.435	–	0.296	–	0.045	–	2.458	–	0.951	0.114	3
0.584	2.024	0.069	2.060	0.011	2.048	0.590	2.122	0.953	0.116	3
0.138	2.041	0.015	2.120	0.003	2.039	0.139	2.111	0.951	0.115	3
0.036	2.023	0.004	2.047	0.001	2.006	0.036	1.961	0.956	0.115	3
0.009	2.148	0.001	2.133	0.000	2.185	0.009	2.011	0.957	0.115	3

Table 5.2: EXAMPLE 1, $\mathbb{P}_1 - \mathbb{RT}_1 - \mathbb{P}_1 - \mathbf{P}_2 - \mathbf{RT}_1 - \mathbf{P}_2$ scheme with quasi-uniform refinement.

N	h	$e(\mathbf{t})$	$r(\mathbf{t})$	$e(\boldsymbol{\sigma})$	$r(\boldsymbol{\sigma})$	$e(\boldsymbol{\rho})$	$r(\boldsymbol{\rho})$	$e(\mathbf{u})$	$r(\mathbf{u})$	$e(p)$	$r(p)$
1803	0.190	1.651	–	485.735	–	2.078	–	2.717	–	11.050	–
6987	0.103	0.692	1.285	540.574	–	1.742	0.260	3.783	–	11.448	–
27345	0.049	1.409	–	384.144	0.501	1.410	0.310	1.625	1.238	6.920	0.738
107985	0.026	1.135	0.315	231.471	0.738	0.932	0.603	0.673	1.285	2.842	1.296
430221	0.013	0.646	0.817	123.634	0.907	0.558	0.742	0.208	1.698	1.205	1.242

$e(\mathbf{p})$	$r(\mathbf{p})$	$e(\theta)$	$r(\theta)$	$e(\boldsymbol{\sigma}_P)$	$r(\boldsymbol{\sigma}_P)$	e	r	$\text{eff}(\Theta_1)$	$\text{eff}(\Theta_2)$	iter
260.136	–	82.410	–	5.521	–	557.149	–	1.010	0.701	8
453.925	–	105.853	–	6.172	–	713.786	–	1.013	0.712	6
338.485	0.430	31.700	1.767	4.031	0.624	512.982	0.484	1.002	0.708	5
221.602	0.617	10.676	1.585	1.674	1.280	320.629	0.684	1.001	0.707	4
125.639	0.821	2.834	1.919	0.970	0.789	176.293	0.865	1.000	0.707	3

Table 5.3: EXAMPLE 2, $\mathbb{P}_0 - \mathbb{RT}_0 - \mathbb{P}_0 - \mathbf{P}_1 - \mathbf{RT}_0 - \mathbf{P}_1$ scheme with quasi-uniform refinement.

N	e(t)	r(t)	e(σ)	r(σ)	e(ρ)	r(ρ)	e(u)	r(u)	e(p)	r(p)
1803	1.651	–	485.735	–	2.078	–	2.717	–	11.050	–
2793	1.152	1.645	477.153	0.042	0.887	3.893	2.440	0.491	5.918	2.854
3969	1.353	–	233.594	3.936	0.604	2.188	0.715	6.984	3.017	3.834
6465	1.108	0.818	95.506	3.515	0.503	0.751	0.524	1.274	2.464	0.829
12177	0.985	0.372	52.350	2.003	0.435	0.460	0.425	0.665	2.127	0.466
24309	0.789	0.641	35.354	1.156	0.358	0.558	0.286	1.139	1.696	0.655
42405	0.612	0.913	26.435	1.043	0.284	0.830	0.173	1.822	1.213	1.204
78363	0.507	0.615	19.354	1.030	0.238	0.581	0.126	1.033	0.957	0.772
148599	0.337	1.276	14.094	1.012	0.173	1.004	0.067	1.976	0.668	1.123
286053	0.268	0.702	10.136	0.989	0.138	0.682	0.047	1.045	0.513	0.807
562743	0.172	1.313	7.245	1.008	0.089	1.287	0.025	1.904	0.324	1.358

e(p)	r(p)	e(θ)	r(θ)	e(σ_P)	r(σ_P)	e	r	eff(Θ_1)	iter
260.136	–	82.410	–	5.521	–	557.149	–	1.010	8
410.800	–	57.315	1.659	3.435	2.169	632.238	–	1.005	5
218.748	3.587	20.780	5.775	2.067	2.891	320.704	3.863	1.003	5
86.491	3.804	19.236	0.317	1.540	1.207	130.284	3.693	1.014	5
42.241	2.264	17.562	0.288	1.316	0.496	69.531	1.984	1.042	5
28.680	1.120	13.182	0.830	1.069	0.601	47.403	1.108	1.052	4
21.095	1.104	10.129	0.947	0.789	1.093	35.311	1.058	1.053	3
15.621	0.978	8.060	0.744	0.642	0.670	26.151	0.978	1.061	3
11.037	1.086	3.787	2.361	0.440	1.184	18.302	1.116	1.025	3
8.051	0.963	2.458	1.320	0.352	0.680	13.179	1.003	1.020	3
5.615	1.065	0.981	2.716	0.228	1.289	9.221	1.056	1.007	3

Table 5.4: EXAMPLE 2, $\mathbb{P}_0 - \mathbb{RT}_0 - \mathbb{P}_0 - \mathbf{P}_1 - \mathbf{RT}_0 - \mathbf{P}_1$ scheme with adaptive refinement via Θ_1 .

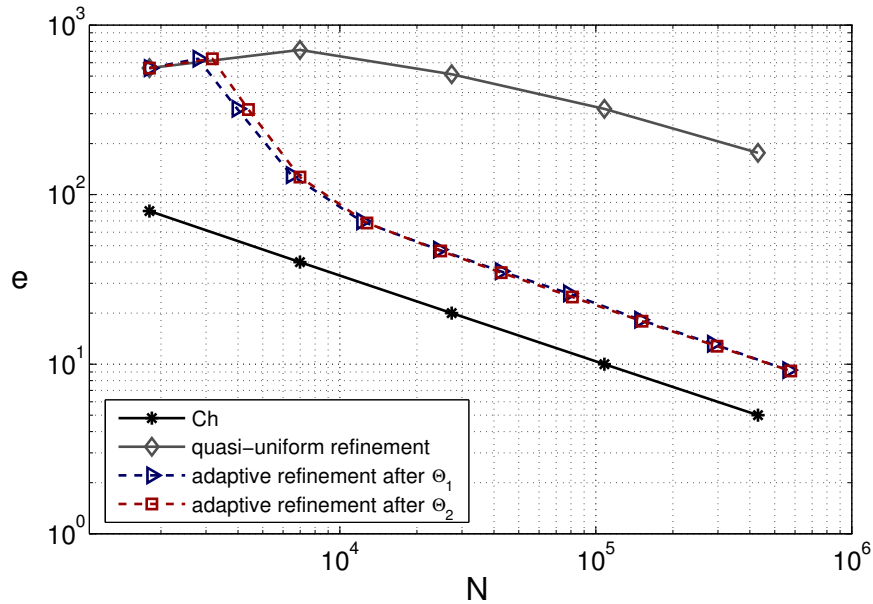


Figure 5.1: Example 2, e vs. N for quasi-uniform/adaptive schemes.

N	e(t)	r(t)	e(σ)	r(σ)	e(ρ)	r(ρ)	e(u)	r(u)	e(p)	r(p)
1803	1.651	–	485.735	–	2.078	–	2.717	–	11.050	–
3177	1.161	1.242	479.666	0.044	0.910	2.914	2.499	0.295	8.074	1.108
4395	1.358	–	233.586	4.434	0.720	1.447	0.688	7.946	2.966	6.170
6987	1.041	1.147	92.836	3.981	0.438	2.147	0.453	1.804	2.021	1.655
12759	0.953	0.230	51.210	1.976	0.374	0.518	0.404	0.384	1.785	0.413
24789	0.715	0.864	34.828	1.161	0.347	0.224	0.227	1.732	1.333	0.878
42729	0.576	0.793	26.799	0.963	0.258	1.091	0.152	1.481	1.070	0.807
81009	0.435	0.879	18.989	1.077	0.218	0.526	0.095	1.469	0.865	0.666
151581	0.319	0.993	14.100	0.950	0.157	1.055	0.055	1.719	0.607	1.131
297489	0.233	0.924	9.898	1.050	0.121	0.757	0.037	1.191	0.444	0.924
577731	0.162	1.093	7.223	0.949	0.078	1.342	0.020	1.901	0.304	1.140

e(p)	r(p)	e(θ)	r(θ)	e(σ_P)	r(σ_P)	e	r	eff(Θ_2)	iter
260.136	–	82.410	–	5.521	–	557.149	–	0.701	8
408.119	–	57.796	1.253	3.587	1.523	632.447	–	0.709	5
214.041	3.977	19.688	6.637	2.312	2.707	317.437	4.248	0.708	5
84.584	4.005	17.847	0.424	1.442	2.038	126.858	3.957	0.712	5
41.294	2.381	17.352	0.093	1.301	0.342	68.044	2.069	0.723	4
28.423	1.125	12.086	1.089	0.955	0.930	46.558	1.143	0.720	4
20.719	1.161	7.255	1.874	0.751	0.885	34.649	1.085	0.715	3
15.350	0.938	4.951	1.195	0.565	0.889	24.919	1.031	0.709	3
10.830	1.113	2.240	2.532	0.422	0.930	17.923	1.052	0.704	3
7.893	0.938	1.568	1.060	0.313	0.883	12.760	1.008	0.699	3
5.517	1.079	0.641	2.697	0.214	1.150	9.113	1.014	0.699	3

Table 5.5: EXAMPLE 2, $\mathbb{P}_0 - \mathbb{RT}_0 - \mathbb{P}_0 - \mathbf{P}_1 - \mathbf{RT}_0 - \mathbf{P}_1$ scheme with adaptive refinement via Θ_2 .

N	h	e(t)	r(t)	e(σ)	r(σ)	e(ρ)	r(ρ)	e(u)	r(u)	e(p)	r(p)
8884	0.354	2.808	–	202.828	–	3.755	–	2.133	–	13.714	–
67396	0.177	2.070	0.451	196.015	0.051	3.701	0.021	2.435	–	8.711	0.672
525316	0.088	1.703	0.285	134.581	0.549	2.871	0.371	1.288	0.930	4.323	1.024
4148740	0.044	1.168	0.548	79.625	0.762	1.811	0.669	0.524	1.307	2.078	1.063

e(p)	r(p)	e(θ)	r(θ)	e(σ_P)	r(σ_P)	e	r	eff(Θ_1)	iter
160.643	–	74.310	–	5.237	–	269.247	–	1.040	7
180.583	–	68.476	0.121	3.958	0.415	275.218	–	1.037	6
121.390	0.580	33.893	1.027	3.120	0.347	184.416	0.585	1.020	5
73.642	0.726	12.062	1.500	1.933	0.695	109.150	0.761	1.007	4

Table 5.6: EXAMPLE 3, $\mathbb{P}_0 - \mathbb{RT}_0 - \mathbb{P}_0 - \mathbf{P}_1 - \mathbf{RT}_0 - \mathbf{P}_1$ scheme with quasi-uniform refinement.

N	e(t)	r(t)	e(σ)	r(σ)	e(ρ)	r(ρ)	e(u)	r(u)	e(p)	r(p)
8884	2.808	–	202.828	–	3.755	–	2.133	–	13.714	–
16760	2.912	–	195.934	0.163	3.105	0.898	1.136	2.978	10.403	1.306
121932	1.913	0.635	135.452	0.558	1.815	0.812	1.051	0.118	5.117	1.073
782480	1.197	0.757	72.896	1.000	1.078	0.841	0.390	1.598	2.536	1.133
4282528	0.649	1.081	36.213	1.235	0.601	1.031	0.161	1.561	1.246	1.255

e(p)	r(p)	e(θ)	r(θ)	e(σ_P)	r(σ_P)	e	r	eff(Θ_1)	iter
160.643	–	74.310	–	5.237	–	269.247	–	1.040	7
163.159	–	32.320	3.935	3.794	1.524	257.051	0.219	1.007	6
120.935	0.453	27.820	0.227	2.455	0.658	183.724	0.508	1.009	5
66.899	0.955	9.073	1.808	1.422	0.881	99.370	0.992	1.004	5
33.902	1.200	3.302	1.784	0.741	1.151	49.724	1.222	1.006	4

Table 5.7: EXAMPLE 3, $\mathbb{P}_0 - \mathbb{RT}_0 - \mathbb{P}_0 - \mathbf{P}_1 - \mathbf{RT}_0 - \mathbf{P}_1$ scheme with adaptive refinement via Θ_1 .

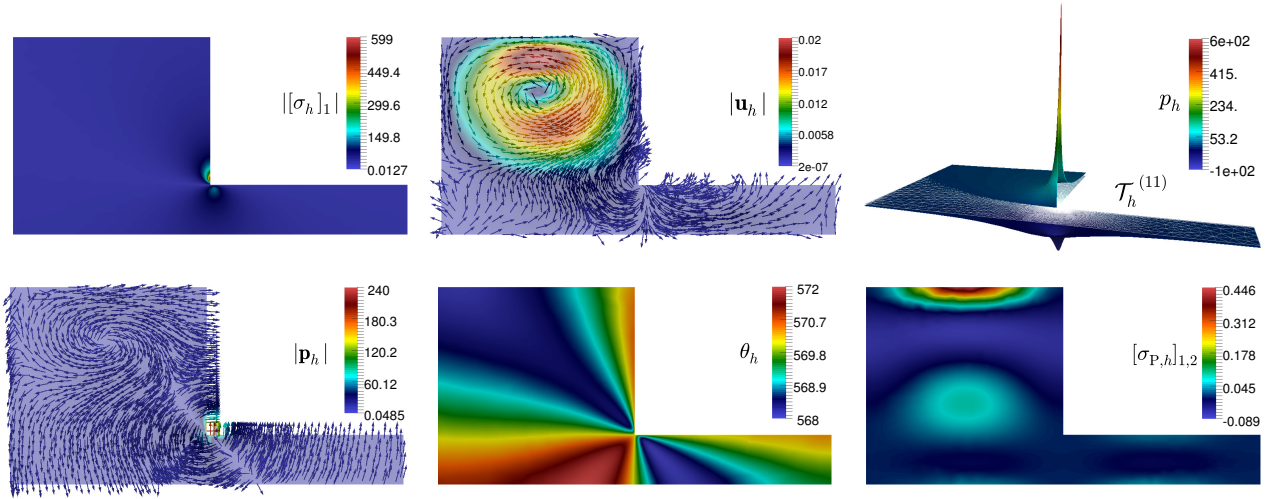


Figure 5.2: Example 2, approximated spectral norm of the stress tensor component, velocity streamlines, and pressure field (top panels), heat flux streamlines, temperature field, and polymeric part of the extra-stress tensor component (bottom panels).

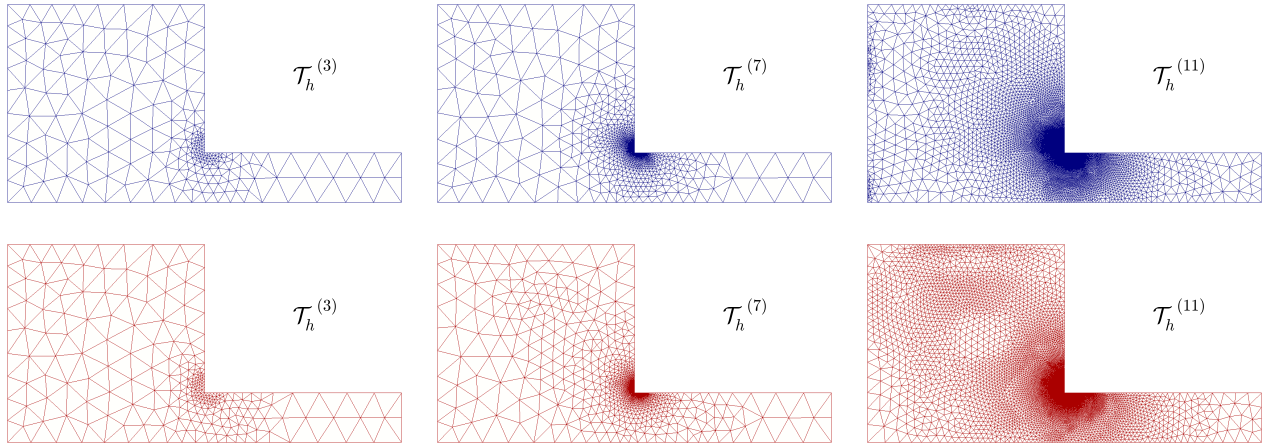


Figure 5.3: Example 2, three snapshots of adapted meshes according to the indicators Θ_1 and Θ_2 (top and bottom panels, respectively).

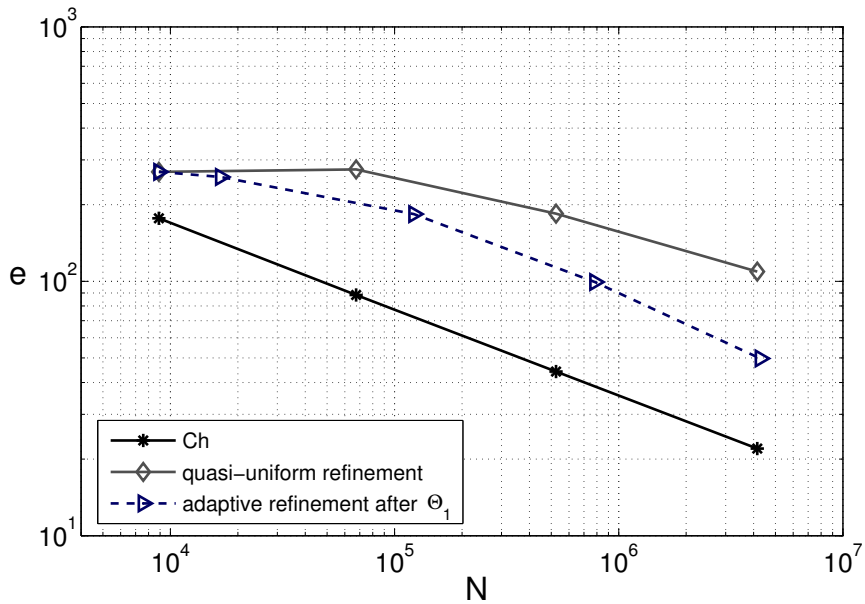


Figure 5.4: Example 3, e vs. N for quasi-uniform/adaptive scheme via Θ_1 .

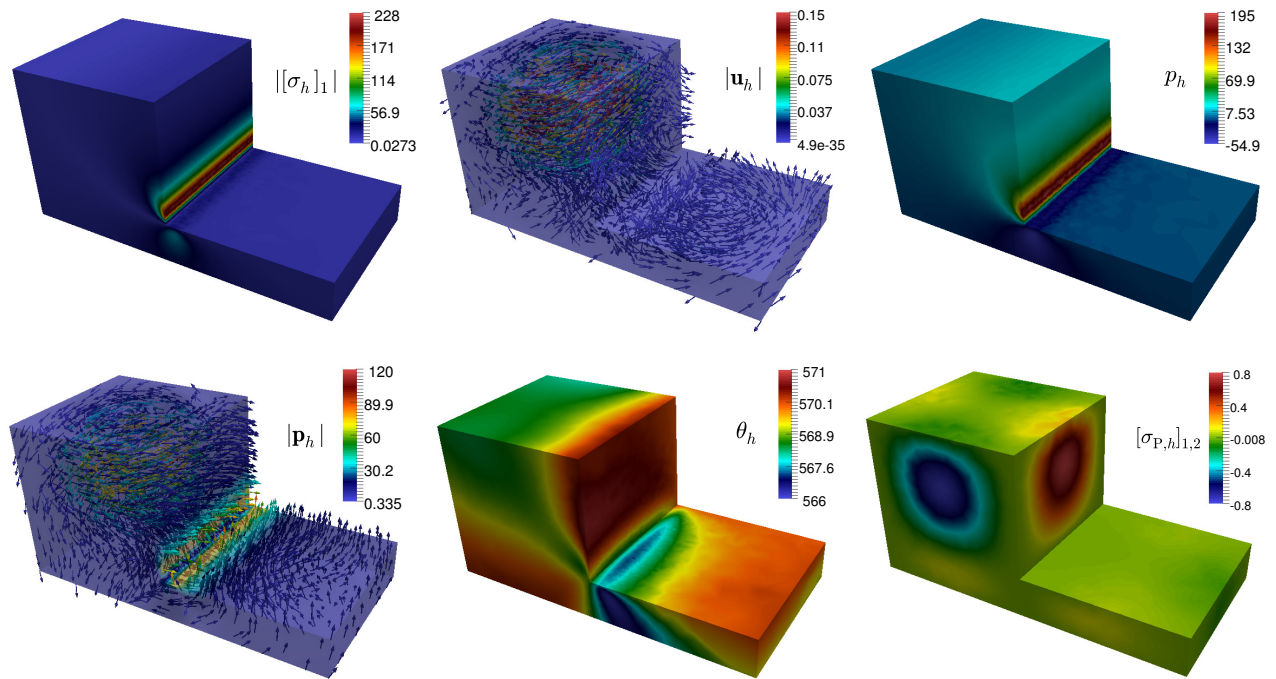


Figure 5.5: Example 3, approximated spectral norm of the stress tensor component, velocity streamlines, and pressure field (top panels), heat flux streamlines, temperature field, and polymeric part of the extra-stress tensor component (bottom panels).

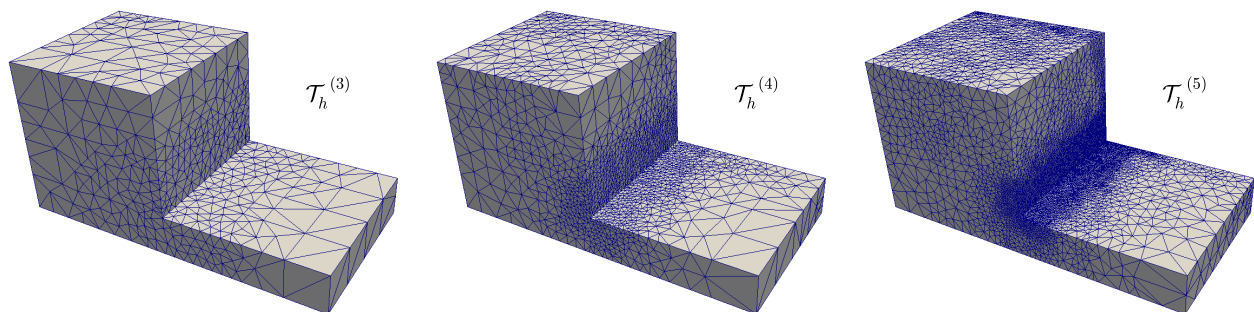


Figure 5.6: Example 3, three snapshots of adapted meshes according to the indicators Θ_1 .

References

- [1] M. ALVAREZ, G.N. GATICA AND R. RUIZ-BAIER, *A posteriori error analysis for a viscous flow-transport problem*. ESAIM Math. Model. Numer. Anal. 50 (2016), no. 6, 1789–1816.
- [2] J. BARANGER AND D. SANDRI, *A formulation of Stokes’s problem and the linear elasticity equations suggested by the Oldroyd model for viscoelastic flow*. RAIRO Modél. Math. Anal. Numér. 26 (1992), no. 2, 331–345.
- [3] T.P. BARRIOS, G.N. GATICA, M. GONZÁLEZ AND N. HEUER, *A residual based a posteriori error estimator for an augmented mixed finite element method in linear elasticity*. M2AN Math. Model. Numer. Anal. 40 (2006), no. 5, 843–869 (2007).
- [4] F. BREZZI AND M. FORTIN, *Mixed and Hybrid Finite Element Methods*. Springer Series in Computational Mathematics, 15. Springer-Verlag, New York, 1991.
- [5] J. CAMAÑO, G.N. GATICA, R. OYARZÚA AND R. RUIZ-BAIER, *An augmented stress-based mixed finite element method for the steady state Navier–Stokes equations with nonlinear viscosity*. Numer. Methods Partial Differential Equations 33 (2017), no. 5, 1692–1725.
- [6] S. CAUCAO, G.N. GATICA AND R. OYARZÚA, *Analysis of an augmented fully-mixed formulation for the non-isothermal Oldroyd–Stokes problem*. Preprint 2017–21, Centro de Investigación de Ingeniería Matemática (CI²MA), Universidad de Concepción, Chile, (2017).
- [7] P. CLÉMENT, *Approximation by finite element functions using local regularisation*. RAIRO Modélisation Mathématique et Analyse Numérique 9 (1975), 77–84.
- [8] E. COLMENARES, G.N. GATICA AND R. OYARZÚA, *Fixed point strategies for mixed variational formulations of the stationary Boussinesq problem*. C. R. Math. Acad. Sci. Paris 354 (2016), no. 1, 57–62.
- [9] E. COLMENARES, G.N. GATICA AND R. OYARZÚA, *Analysis of an augmented mixed-primal formulation for the stationary Boussinesq problem*. Numer. Methods Partial Differential Equations 32 (2016), no. 2, 445–478.
- [10] E. COLMENARES, G.N. GATICA AND R. OYARZÚA, *An augmented fully-mixed finite element method for the stationary Boussinesq problem*. Calcolo 54 (2017), no. 1, 167–205.
- [11] E. COLMENARES, G.N. GATICA AND R. OYARZÚA, *A posteriori error analysis of an augmented mixed-primal formulation for the stationary Boussinesq model*. Calcolo 54 (2017), no. 3, 1055–1095.
- [12] E. COLMENARES, G.N. GATICA AND R. OYARZÚA, *A posteriori error analysis of an augmented fully-mixed formulation for the stationary Boussinesq model*. Preprint 2017–17, Centro de Investigación de Ingeniería Matemática (CI²MA), Universidad de Concepción, Chile, (2017).
- [13] C. COX, H. LEE AND D. SZURLEY, *Finite element approximation of the non-isothermal Stokes–Oldroyd equations*. Int. J. Numer. Anal. Model. 4 (2007), no. 3-4, 425–440.
- [14] C. COX, H. LEE AND D. SZURLEY, *Optimal control of non-isothermal viscous fluid flow*. Math. Comput. Modelling 50 (2009), no. 7-8, 1142–1153.

- [15] C. DOMÍNGUEZ, G.N. GATICA AND S. MEDDAHI, *A posteriori error analysis of a fully-mixed finite element method for a two-dimensional fluid-solid interaction problem*. J. Comput. Math. 33 (2015), no. 6, 606–641.
- [16] A. ERN AND J.-L. GUERMOND, *Theory and Practice of Finite Elements*. Applied Mathematical Sciences, 159. Springer-Verlag, New York, 2004.
- [17] V.J. ERVIN AND L.N. NTASIN, *A posteriori error estimation and adaptive computation of viscoelastic fluid flow*. Numer. Methods Partial Differential Equations 21 (2005), no. 2, 297–322.
- [18] M. FARHLOUL AND A. ZINE, *A dual mixed formulation for non-isothermal Oldroyd–Stokes problem*. Math. Model. Nat. Phenom. 6 (2011), no. 5, 130–156.
- [19] J.R. FERNÁNDEZ AND P. HILD, *A priori and a posteriori error analyses in the study of viscoelastic problems*. J. Comput. Appl. Math. 225 (2009), no. 2, 569–580.
- [20] J.R. FERNÁNDEZ AND D. SANTAMARINA, *An a posteriori error analysis for dynamic viscoelastic problems*. ESAIM Math. Model. Numer. Anal. 45 (2011), no. 5, 925–945.
- [21] G.N. GATICA, *A Simple Introduction to the Mixed Finite Element Method. Theory and Applications*. Springer Briefs in Mathematics. Springer, Cham, 2014.
- [22] G.N. GATICA, *A note on stable Helmholtz decompositions in 3D*. Preprint 2016–03, Centro de Investigación de Ingeniería Matemática (CI²MA), Universidad de Concepción, Chile, (2016).
- [23] G.N. GATICA, G.C. HSIAO AND S. MEDDAHI, *A residual-based a posteriori error estimator for a two-dimensional fluid-solid interaction problem*. Numer. Math. 114 (2009), no. 1, 63–106.
- [24] G.N. GATICA, A. MÁRQUEZ AND M.A. SÁNCHEZ, *A priori and a posteriori error analyses of a velocity-pseudostress formulation for a class of quasi-Newtonian Stokes flows*. Comput. Methods Appl. Mech. Engrg. 200 (2011), no. 17-20, 1619–1636.
- [25] G.N. GATICA, R. RUIZ-BAIER AND G. TIERRA, *A posteriori error analysis of an augmented mixed method for the Navier–Stokes equations with nonlinear viscosity*. Comput. Math. Appl. 72 (2016), no. 9, 2289–2310.
- [26] V. GIRAULT AND P.-A. RAVIART, *Finite Element Methods for Navier–Stokes Equations. Theory and Algorithms*. Springer Series in Computational Mathematics, 5. Springer-Verlag, Berlin, 1986.
- [27] F. HECHT, *New development in FreeFem++*. J. Numer. Math. 20 (2012), no. 3-4, 251–265.
- [28] Y.L. JOO, J. SUN, M.D. SMITH, R.C. ARMSTRONG AND R.A. ROSS, *Two-dimensional numerical analysis of non-isothermal melt spinning with and without phase transition*. J. Non-Newtonian Fluid Mech. 102 (2002), no. 1, 37–70.
- [29] K. NAJIB, D. SANDRI AND A.-M. ZINE, *On a posteriori estimates for a linearized Oldroyd’s problem*. J. Comput. Appl. Math. 167 (2004), no. 2, 345–361.
- [30] M. PICASSO AND J. RAPPAZ, *Existence, a priori and a posteriori error estimates for a nonlinear three-field problem arising from Oldroyd-B viscoelastic flows*. M2AN Math. Model. Numer. Anal. 35 (2001), no. 5, 879–897.

Centro de Investigación en Ingeniería Matemática (CI²MA)

PRE-PUBLICACIONES 2017

- 2017-14 MARIO ÁLVAREZ, GABRIEL N. GATICA, RICARDO RUIZ-BAIER: *A posteriori error analysis of a fully-mixed formulation for the Brinkman-Darcy problem*
- 2017-15 DANIELE BOFFI, LUCIA GASTALDI, RODOLFO RODRÍGUEZ, IVANA SEBESTOVA: *A posteriori error estimates for Maxwell eigenvalue problem*
- 2017-16 GABRIEL N. GATICA: *A note on weak* convergence and compactness and their connection to the existence of the inverse-adjoint*
- 2017-17 ELIGIO COLMENARES, GABRIEL N. GATICA, RICARDO OYARZÚA: *A posteriori error analysis of an augmented fully-mixed formulation for the stationary Boussinesq model*
- 2017-18 JAVIER A. ALMONACID, GABRIEL N. GATICA, RICARDO OYARZÚA: *A mixed-primal finite element method for the Boussinesq problem with temperature-dependent viscosity*
- 2017-19 RAIMUND BÜRGER, ILJA KRÖKER: *Computational uncertainty quantification for some strongly degenerate parabolic convection-diffusion equations*
- 2017-20 GABRIEL N. GATICA, BRYAN GOMEZ-VARGAS, RICARDO RUIZ-BAIER: *Mixed-primal finite element methods for stress-assisted diffusion problems*
- 2017-21 SERGIO CAUCAO, GABRIEL N. GATICA, RICARDO OYARZÚA: *Analysis of an augmented fully-mixed formulation for the non-isothermal Oldroyd-Stokes problem*
- 2017-22 ROLANDO BISCAY, JOAQUIN FERNÁNDEZ, CARLOS M. MORA: *Numerical solution of stochastic master equations using stochastic interacting wave functions*
- 2017-23 GABRIEL N. GATICA, MAURICIO MUNAR, FILANDER A. SEQUEIRA: *A mixed virtual element method for the Navier-Stokes equations*
- 2017-24 NICOLAS BARNAFI, GABRIEL N. GATICA, DANIEL E. HURTADO: *Primal and mixed finite element methods for deformable image registration problems*
- 2017-25 SERGIO CAUCAO, GABRIEL N. GATICA, RICARDO OYARZÚA: *A posteriori error analysis of an augmented fully-mixed formulation for the non-isothermal Oldroyd-Stokes problem*

Para obtener copias de las Pre-Publicaciones, escribir o llamar a: DIRECTOR, CENTRO DE INVESTIGACIÓN EN INGENIERÍA MATEMÁTICA, UNIVERSIDAD DE CONCEPCIÓN, CASILLA 160-C, CONCEPCIÓN, CHILE, TEL.: 41-2661324, o bien, visitar la página web del centro: <http://www.ci2ma.udec.cl>



**CENTRO DE INVESTIGACIÓN EN
INGENIERÍA MATEMÁTICA (CI²MA)
Universidad de Concepción**



Casilla 160-C, Concepción, Chile
Tel.: 56-41-2661324/2661554/2661316
<http://www.ci2ma.udec.cl>

